

AD-A081 255

VIRGINIA POLYTECHNIC INST AND STATE UNIV BLACKSBURG --EYE F/6 20/4
ON GOERTLER INSTABILITY.(U)

DEC 79 S A RAGAB, A H MAYFEH

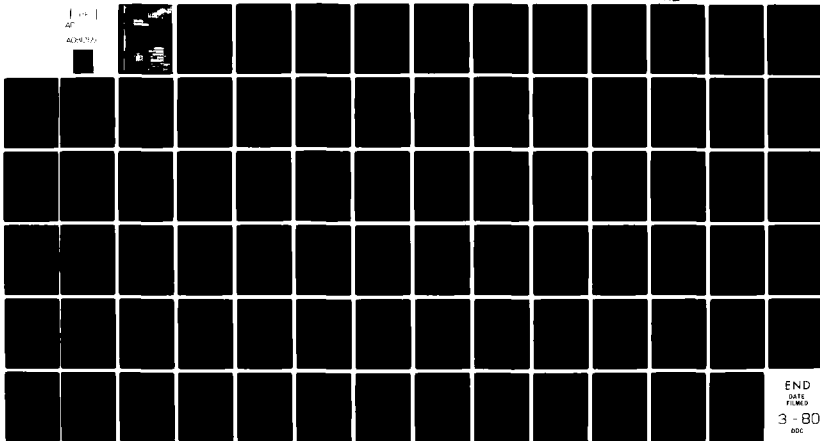
N00014-75-C-0381

UNCLASSIFIED

VPI-E-79-41

NL

1 1/2
AD-A081 255



END
DATE
FILMED
3-80
RSC

LEVEL # ①

⑭ VPI-E-79-41

⑮ Contract N00014-75-C-0381

⑥ On Görtler Instability.

by

⑩ Saad Aly/Ragab and Ali Hasan/Nayfeh

⑨ March, Rept. 4

⑪ Dec. 77

⑫ 81

Engineering Science and Mechanics Department
Virginia Polytechnic Institute and State University
Blacksburg, VA 24061

DTIC
ELECTE
FEB 27 1980

A

DISTRIBUTION STATEMENT A

Approved for public release;
Distribution Unlimited

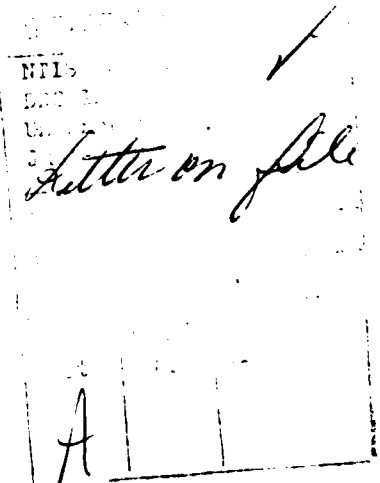
404722

On Görtler Instability

Saad Aly Ragab and Ali Hasan Nayfeh

Department of Engineering Science and Mechanics
Virginia Polytechnic Institute and State University
Blacksburg, Virginia 24061

Görtler instability for boundary-layer flows over generally curved walls is considered. The full linearized disturbance equations are obtained in an orthogonal curvilinear coordinate system. A perturbation procedure to account for second-order effects is used to determine the effects of the displacement thickness and the variation of the stream-line curvature on the neutral stability of the Blasius flow. The pressure gradient in the mean flow is accounted for by solving the non-similar boundary-layer equations. Growth rates are obtained for the actual mean flow and compared with those for the Blasius flow and the Falkner-Skan flows. The results demonstrate the strong influence of the pressure gradient and the nonsimilarity of the basic flow on the stability characteristics.



On Görtler Instability

Saad Aly Ragab and Ali Hasan Nayfeh

Department of Engineering Science and Mechanics
Virginia Polytechnic Institute and State University
Blacksburg, Virginia 24061

I. Introduction

Centrifugal instability in boundary-layer flows over concavely curved walls was first demonstrated theoretically by Görtler¹. The disturbances are in the form of counter-rotating streamwise vortices, called Görtler vortices. Wortman² gave a detailed flow visualization of these vortices on slightly curved walls. Bippes³ conducted experiments on walls with radii of 0.5 and 1.0m so that the generated vortices were fairly strong.

These vortices by themselves may not lead to the transition of laminar flows to turbulent flows. The influence of steady streamwise vortices on two-dimensional Tollmien-Schlichting waves was studied experimentally by Aihara⁴, Tani and Sakagami⁵, and Tani and Aihara⁶. They concluded that the Görtler vortices indirectly affect the transition by inducing a spanwise variation in boundary-layer thickness, at least when the radii of curvature are not extremely small. After reviewing the experimental work on the subject, Nayfeh⁷ presented a theoretical model for studying the effect of streamwise vortices on Tollmien-Schlichting waves. He showed that such vortices have a strong tendency to amplify three-dimensional Tollmien-Schlichting waves having a spanwise wavelength that is twice the wavelength of the vortices. Therefore, the study of Görtler instability is of importance not only in

heat exchange problems but also in the analysis of the transition region over concavely curved walls.

Improvements and extensions of the Görtler model were considered by many authors. Hämmerlin^{8,9} relaxed some of the assumptions made by Görtler regarding the treatment of the curvature terms. He⁹ accounted for the variation of the streamline curvature normal to the wall by using a flow that has the properties of boundary-layer flows along a wavy wall in the valley positions. For these flows, the streamline curvature decays exponentially away from the wall. Tobak¹⁰ considered the case of a wall having a finite extent of streamwise curvature. The effect of this curvature in the final equations appears as a multiplier to the Görtler number. Herbert¹¹ gave a comprehensive survey of the effort of these authors and obtained very accurate numerical solutions to their models.

Smith¹² incorporated the transverse component of the basic flow and some of the higher-order curvature terms. Furthermore, he considered spatially rather than temporally growing vortices. Smith's viewpoint is consistent with the experimental observations. Smith used body-oriented axes and a Taylor-series expansion of the metric coefficient for small distances normal to the wall. He kept two terms in the expansion. A complete survey and critical discussion of the role of the coordinate system in the Görtler problem was given by Floryan and Saric¹³. They reformulated the problem in an orthogonal curvilinear coordinate system constructed from the potential- and stream-lines of the inviscid flow over the curved wall. They pointed out how this coordinate system overcomes the singularity in the metric coefficient associated with

body-oriented axes. They considered the case of a circular arc and obtained the basic approximations of the mean-flow and disturbance equations. They concluded that the correct zeroth-order base flow for the stability analysis is the Blasius flow. They based the scaling of the disturbance in the transverse component on a viscous scale, namely ν/δ_r , where ν is the kinematic viscosity and δ_r is a reference boundary-layer thickness. As a result of this ordering, the transverse component of the basic flow has a first-order effect on the stability analysis. This fact was also pointed out by Herbert¹¹ after introducing the Görtler number into Smith's equations. Moreover, the streamwise variation of the transverse component of the basic flow appears also in the first-order equations. This term, which has a strong influence on the stability characteristics (in particular the neutral stability curve), is missing from the analyses preceding that of Floryan and Saric¹³.

Here, we are interested in flow over walls with general distributions of curvature. Specifically, we consider the effect of the streamwise pressure gradient on the stability characteristics. Following Floryan and Saric¹³, we employ a coordinate system based on the potential- and stream-lines. The inviscid flow and the metric coefficients of the coordinate system are obtained by the method of Davis¹⁴ for constructing body-fitted coordinate systems. His method is based on the Schwarz-Christoffel transformation generalized for curved surfaces. In Section II, the two-dimensional basic-flow equations are derived in a general orthogonal curvilinear coordinate system. The obtained equations are specialized for body-oriented axes and for potential- and stream-line coordinates. In Section III, the complete linearized Navier-Stokes

equations are derived for the disturbance quantities. The quasi-parallel-flow assumption and the normal-mode solution are discussed. Then a method of solution is presented. Terms of order smaller than $O(1)$ are treated as perturbation quantities to a basic system that includes the $O(1)$ terms. The method of solution of the basic system is presented in Section IV. A new method of applying the asymptotic boundary condition far from the wall is presented. In Section V, a perturbation procedure is presented to account for the small quantities in the disturbance equations. Results and their discussion are presented in Section VI.

II. The Basic Flow

We consider steady two-dimensional viscous incompressible flows over a curved wall. The fluid properties ρ^* and μ^* are assumed to be constants. Following Floryan and Saric¹³, we employ an orthogonal curvilinear coordinate system ϕ^* , ψ^* , and z^* . Later, we identify ϕ^* and ψ^* as the potential and stream functions of the two-dimensional inviscid flow over the given wall, respectively, and z^* as a rectilinear coordinate normal to the plane of the basic motion, see Fig. 1. The Navier-Stokes equations in this coordinate system are given in Appendix A. We introduce the following nondimensional variables:

$$\phi = \phi^*/U_\infty^*L^*, \quad \psi = \psi^*/U_\infty^*L^* \quad (1)$$

$$h_\phi = h_\phi^*U_\infty^*, \quad h_\psi = h_\psi^*U_\infty^* \quad (2)$$

$$u = u^*/U_\infty^*, \quad v = v^*/U_\infty^*, \quad w = w^*/U_\infty^*, \quad p = p^*/\rho^*U_\infty^{*2} \quad (3)$$

We define a characteristic Reynolds number $Re = \rho^*U_\infty^*L^*/\mu^*$, where U_∞^* , ρ^* , and μ^* are the free-stream values of velocity, density, and

viscosity and L^* is a characteristic length, the distance from the leading edge of the curved wall to the position of maximum height, see Fig. 2.

The equations of Appendix A for the two-dimensional case (i.e., $w = 0$, $\partial/\partial z = 0$) become

ϕ -Momentum Equation

$$\begin{aligned} \frac{u}{h_\phi} \frac{\partial u}{\partial \phi} + \frac{v}{h_\psi} \frac{\partial u}{\partial \psi} - \frac{v^2}{h_\phi h_\psi} \frac{\partial h_\psi}{\partial \phi} + \frac{uv}{h_\phi h_\psi} \frac{\partial h_\phi}{\partial \psi} + \frac{1}{h_\phi} \frac{\partial p}{\partial \phi} = \frac{1}{\text{Re}} \frac{1}{h_\phi h_\psi} \left\{ \frac{\partial}{\partial \phi} \left(2 \frac{h_\psi}{h_\phi} \frac{\partial u}{\partial \phi} \right. \right. \\ \left. \left. + 2 \frac{v}{h_\phi} \frac{\partial h_\phi}{\partial \psi} \right) + \frac{\partial}{\partial \psi} \left[h_\psi \frac{\partial}{\partial \phi} \left(\frac{v}{h_\psi} \right) + \frac{h_\phi^2}{h_\psi} \frac{\partial}{\partial \psi} \left(\frac{u}{h_\phi} \right) \right] + \left[\frac{h_\psi}{h_\phi} \frac{\partial}{\partial \phi} \left(\frac{v}{h_\psi} \right) \right. \right. \\ \left. \left. + \frac{h_\phi}{h_\psi} \frac{\partial}{\partial \psi} \left(\frac{u}{h_\phi} \right) \right] \frac{\partial h_\phi}{\partial \psi} - 2 \left(\frac{1}{h_\psi} \frac{\partial v}{\partial \psi} + \frac{u}{h_\phi h_\psi} \frac{\partial h_\psi}{\partial \phi} \right) \frac{\partial h_\psi}{\partial \phi} \right\} \quad (4) \end{aligned}$$

ψ -Momentum Equation

$$\begin{aligned} \frac{u}{h_\phi} \frac{\partial v}{\partial \phi} + \frac{v}{h_\psi} \frac{\partial v}{\partial \psi} + \frac{uv}{h_\phi h_\psi} \frac{\partial h_\psi}{\partial \phi} - \frac{u^2}{h_\phi h_\psi} \frac{\partial h_\phi}{\partial \psi} + \frac{1}{h_\psi} \frac{\partial p}{\partial \psi} = \frac{1}{\text{Re}} \frac{1}{h_\phi h_\psi} \left\{ \frac{\partial}{\partial \phi} \left[\frac{h_\psi^2}{h_\phi} \frac{\partial}{\partial \phi} \left(\frac{v}{h_\psi} \right) \right. \right. \\ \left. \left. + h_\phi \frac{\partial}{\partial \psi} \left(\frac{u}{h_\phi} \right) \right] + \frac{\partial}{\partial \psi} \left(2 \frac{h_\phi}{h_\psi} \frac{\partial v}{\partial \psi} + 2 \frac{u}{h_\psi} \frac{\partial h_\psi}{\partial \phi} \right) + \left[\frac{h_\psi}{h_\phi} \frac{\partial}{\partial \phi} \left(\frac{v}{h_\psi} \right) \right. \right. \\ \left. \left. + \frac{h_\phi}{h_\psi} \frac{\partial}{\partial \psi} \left(\frac{u}{h_\phi} \right) \right] \frac{\partial h_\psi}{\partial \phi} - 2 \left[\frac{1}{h_\phi} \frac{\partial u}{\partial \phi} + \frac{v}{h_\phi h_\psi} \frac{\partial h_\phi}{\partial \psi} \right] \frac{\partial h_\phi}{\partial \psi} \right\} \quad (5) \end{aligned}$$

Continuity Equation

$$\frac{\partial}{\partial \phi} (h_\psi u) + \frac{\partial}{\partial \psi} (h_\phi v) = 0 \quad (6)$$

We assume that the metric coefficients h_ϕ and h_ψ and their derivatives that appear in Eqs. (4)-(6) are all $O(1)$ or less. Hence, regions of severe or discontinuous curvature are excluded.

Following Prandtl, we introduce the stretched variable

$$\bar{\psi} = \text{Re}^{1/2} \psi \quad (7)$$

Then, it follows from Eq. (6), that v must be $O(\text{Re}^{-1/2})$ in the least-degenerate limit. Hence, we let

$$\bar{v} = \text{Re}^{1/2} v \quad (8)$$

where $\bar{v} = O(1)$. Substituting Eqs. (7) and (8) into Eq. (4) and neglecting terms $O(\text{Re}^{-1})$ we obtain, in terms of the unstretched variables,

$$\begin{aligned} \frac{u}{h_\phi} \frac{\partial u}{\partial \phi} + \frac{v}{h_\psi} \frac{\partial u}{\partial \psi} + \frac{uv}{h_\phi h_\psi} \frac{\partial h_\phi}{\partial \psi} + \frac{1}{h_\phi} \frac{\partial p}{\partial \phi} = \frac{1}{\text{Re}} \frac{1}{h_\phi h_\psi} \left\{ \frac{\partial}{\partial \psi} \left[\frac{h_\phi^2}{h_\psi} \frac{\partial}{\partial \psi} \left(\frac{u}{h_\phi} \right) \right] \right. \\ \left. + \frac{h_\phi}{h_\psi} \frac{\partial}{\partial \psi} \left(\frac{u}{h_\phi} \right) \frac{\partial h_\phi}{\partial \psi} \right\} \end{aligned} \quad (9)$$

Similarly, the ψ -momentum equation reduces to

$$\frac{u^2}{h_\phi} \frac{\partial h_\phi}{\partial \psi} = \frac{\partial p}{\partial \psi} \quad (10)$$

The continuity equation is unchanged.

A. Body-Oriented Axes

For a body-oriented axes we identify ϕ as x , the arc length measured along the body contour, and ψ as y , the normal to that contour. Hence

$$h_\phi = 1 + k(x)y \quad (11)$$

$$h_\psi = 1 \quad (12)$$

where $k(x)$ is the local curvature of the contour. Now, Eqs. (9), (10), and (6) become

$$\begin{aligned} \frac{u}{1+ky} \frac{\partial u}{\partial x} + v \frac{\partial u}{\partial y} + \frac{kuv}{1+ky} + \frac{1}{1+ky} \frac{\partial p}{\partial x} = \frac{1}{\text{Re}} \left[\frac{\partial^2 u}{\partial y^2} + \frac{k}{1+ky} \frac{\partial u}{\partial y} \right. \\ \left. - \frac{k^2 u}{(1+ky)^2} \right] \end{aligned} \quad (13)$$

$$\frac{ku^2}{1 + ky} = \frac{\partial p}{\partial y} \quad (14)$$

$$\frac{\partial u}{\partial x} + \frac{\partial}{\partial y} [(1 + ky)v] = 0 \quad (15)$$

Equations (13)-(14) have been derived by Schultz-Grunow and Breuer¹⁵, among many others (see Van Dyke¹⁶ for a complete review), as an appropriate set of equations to describe boundary-layer flows with second-order curvature effects.

B. Equations in Potential and Stream-Lines

Here, we identify ϕ and ψ as the potential and stream functions for the inviscid irrotational flow over the given wall. Furthermore, we choose $\psi = 0$ to coincide with the body surface and $\phi = 0$ to coincide with the leading edge. It follows from the definitions of h_ϕ and h_ψ that

$$h_\phi = h_\psi = 1/U(\phi, \psi) \equiv h \quad (16)$$

where U is the magnitude of the inviscid velocity. Actually, it is the ϕ -component of the velocity since the velocity normal to a streamline is by definition equal to zero. From the irrotationality condition we obtain

$$k_\psi = -\frac{1}{h^2} \frac{\partial h}{\partial \psi} \quad (17)$$

and from the incompressibility condition we obtain

$$k_\phi = \frac{1}{h^2} \frac{\partial h}{\partial \phi} \quad (18)$$

where k_ψ and k_ϕ are the local values of the curvature of a streamline and an equipotential line, respectively.

In this coordinate system, Eqs. (9), (10), and (6) become

$$hu \frac{\partial u}{\partial \phi} + hv \frac{\partial u}{\partial \psi} + uv \frac{\partial h}{\partial \psi} = -h \frac{\partial p}{\partial \phi} + \frac{1}{Re} \frac{\partial^2 u}{\partial \psi^2} \quad (19)$$

$$\frac{u^2}{h} \frac{\partial h}{\partial \psi} = \frac{\partial p}{\partial \psi} \quad (20)$$

$$\frac{\partial}{\partial \phi} (hu) + \frac{\partial}{\partial \psi} (hv) = 0 \quad (21)$$

where the term $\frac{u}{Re} \frac{\partial^2 h}{\partial \psi^2}$ was neglected from Eq. (19) since it is $O(Re^{-1})$, consistent with our assumption that the metric coefficients and their derivatives are $\leq O(1)$. Equations (19)-(21) are alternatives to Eqs. (13)-(15) of the body-oriented axes.

We identify two types of curvature effects on the basic state. The first is a viscous effect that manifests itself through the terms $uv\partial h/\partial \psi$ in Eq. (19) and $(u^2/h)\partial h/\partial \psi$ in Eq. (20). As shown by Van Dyke, this effect is a local one. The second is an inviscid effect that manifests itself in the pressure gradient term $\partial p/\partial \phi$. Since in subsonic flows this effect is a global one, it depends on the distribution of the surface curvature everywhere. Consider for example the flow over the hump shown in Fig. 2. The central part of the hump has an appreciable curvature, specifically, a curvature of $O(1)$, while the upstream part of the hump has a negligible curvature, say $O(Re^{-1/2})$. Nevertheless, the pressure gradient $\partial p/\partial \phi$ in the latter region may not be negligible. One of the main purposes of the present paper is to evaluate the influence of this pressure gradient on the stability characteristics of Görtler vortices. Hence, for this purpose, we neglect the viscous effect of curvature on the basic state because it is a local effect.

We introduce the new variables

$$\tilde{u} = hu \quad (22)$$

$$\tilde{v} = hv \quad (23)$$

Substituting Eq. (22) and (23) into Eqs. (19)-(21) and neglecting terms of order $Re^{-1/2}$, we obtain

$$\tilde{u} \frac{\partial \tilde{u}}{\partial \phi} + \tilde{v} \frac{\partial \tilde{u}}{\partial \psi} = \frac{1}{h} \frac{\partial h}{\partial \phi} (\tilde{u}^2 - 1) + \frac{1}{Re} \frac{\partial^2 \tilde{u}}{\partial \psi^2} \quad (24)$$

$$\frac{\partial p}{\partial \psi} = 0 \quad (25)$$

$$\frac{\partial \tilde{u}}{\partial \phi} + \frac{\partial \tilde{v}}{\partial \psi} = 0 \quad (26)$$

The relation $h^2 \frac{\partial p}{\partial \phi} = \frac{1}{h} \frac{\partial h}{\partial \phi}$, which is valid for the inviscid flow, has been used.

Now, we introduce the Levey-Lees variables

$$\xi = \phi \quad (27)$$

$$\eta = \frac{\psi \sqrt{Re}}{\sqrt{2\xi}} \quad (28)$$

$$F = \tilde{u} \quad (29)$$

$$V = \tilde{v} \sqrt{Re} \sqrt{2\xi} - \eta F \quad (30)$$

Then the ϕ -momentum and the continuity equations take the standard form

$$2\xi F F_{\xi} + V F_{\eta} + \beta_0 (F^2 - 1) - F_{\eta\eta} = 0 \quad (31)$$

$$2\xi F_{\xi} + V_{\eta} + F = 0 \quad (32)$$

where

$$\beta_0 = - \frac{2\xi}{h} \frac{\partial h}{\partial \phi} \quad (33)$$

is a function of ϕ and ψ . However, its deviation from the value at the surface (i.e., at $\psi = 0$) is $O(Re^{-1/2})$ and hence we evaluate it from

$$\beta_0 = - \frac{2\xi}{h(\phi, 0)} \left. \frac{\partial h}{\partial \phi} \right|_{\psi = 0} \quad (34)$$

The boundary conditions for Eqs. (31) and (32) are

$$F = 0, \quad V = 0 \quad \text{at} \quad \eta = 0 \quad (35)$$

and

$$F \rightarrow 1 \quad \text{as} \quad \eta \rightarrow \infty \quad (36)$$

The initial condition is

$$F = F(\xi_0, \eta) \quad \text{at} \quad \xi = \xi_0 \quad (37)$$

In the present application, the initial profile is taken to be the Blasius profile and it is specified at $\xi = 0$. This is because the curved wall approaches a horizontal flat plate near its leading edge.

C. The Inviscid Flow

As an example, we consider a curved wall given by

$$y^* = H^* \operatorname{sech}[B(1 - \frac{x^*}{L^*})] \quad \text{for} \quad |x^*| < \infty \quad (38)$$

where H^* is the maximum height and B is a constant. The curvature variation of this wall is shown in Fig. 3 as a function of x^*/L^* . Equation (38) shows that y^* decays exponentially as $x^* \rightarrow \pm\infty$. For moderate values of B (about 10), $y^*/H^* \approx 2e^{-10}$ at $x^* = 0$, which is very small. Therefore, for the purpose of calculating the inviscid flow over the hump, we assume that the wall is specified by Eq. (38) in the interval $0 \leq x^*/L^* \leq 2$ and it coincides with the x^* -axis outside this interval.

Davis¹⁴ developed an accurate numerical method for integrating Schwartz-Christoffel transformations generalized for curved surfaces. We employ Davis' method to find a function $f(\zeta)$ which maps the upper half of the ζ -plane onto the region above the curved wall in the z -plane. A uniform flow parallel to the ξ -axis in the ζ -plane is transformed into a flow over the hump in the physical plane. Far from the hump the flow returns to a uniform stream. The paper by Davis¹⁴ contains sufficient information for programming the method. However, application of Davis' method to the wall treated in the present work is included in Appendix B.

D. A Method For Solving The Basic Flow Equations

Once β_0 is determined from the inviscid flow solution, then the solution of Eqs. (31) and (32) subject to the boundary and initial conditions, Eqs. (35)-(37), is obtained by using a finite-difference marching technique. A second-order accurate scheme is employed. A Newton-Raphson process is used to quasi-linearize the nonlinear terms in the momentum equation. Hence, the momentum and continuity equations are coupled in their linearized forms. This is known as the Davis coupled scheme (see Blottner¹⁷). The ξ -derivative is replaced by a 3-point backward formula while the η -derivatives are represented by central differences. At the first two streamwise locations, the profiles are taken to be the Blasius profile.

For the Falkner-Skan flows, β_0 is a constant and a self-similar solution for Eqs. (31) and (32) can be obtained. Since the equations are ordinary- rather than partial-differential equations, we use a fourth-order Runge-Kutta method coupled with a shooting technique to satisfy the two-point boundary conditions (35) and (36). The

asymptotic condition (36) is satisfied at $\eta = 18$, which proved to be sufficiently large. The step size $\Delta\eta$ is taken to be 0.01 for all the numerical results presented in this paper.

The basic-flow quantities that appear as coefficients in the perturbation equations of the next section are

$$hu = F \quad (39a)$$

$$\frac{\partial hu}{\partial \psi} = \frac{\partial F}{\partial \eta} \cdot \frac{\partial \eta}{\partial \psi} = \frac{\sqrt{Re}}{\sqrt{2}\phi} \frac{\partial F}{\partial \eta} \quad (39b)$$

$$hv = \frac{V + \eta F}{\sqrt{2Re\phi}} \quad (39c)$$

$$\frac{\partial hv}{\partial \psi} = \frac{\partial hv}{\partial \eta} \cdot \frac{\partial \eta}{\partial \psi} = \frac{1}{2\phi} \frac{\partial}{\partial \eta} (V + \eta F) \quad (39d)$$

$$\begin{aligned} \frac{\partial hv}{\partial \phi} = \frac{\partial hv}{\partial \xi} \frac{\partial \xi}{\partial \phi} + \frac{\partial hv}{\partial \eta} \frac{\partial \eta}{\partial \phi} = \frac{1}{2\sqrt{2Re}} \frac{1}{\phi^{3/2}} [- (V + \eta F) - \eta \frac{\partial}{\partial \eta} (V + \eta F) \\ + 2\xi \frac{\partial}{\partial \xi} (V + \eta F)] \end{aligned} \quad (39e)$$

For further reference we define

$$U_0 \equiv hu = F \quad (40a)$$

$$E_0 \equiv \frac{\sqrt{\phi}}{\sqrt{Re}} \frac{\partial hu}{\partial \psi} = \frac{1}{\sqrt{2}} \frac{\partial F}{\partial \eta} \quad (40b)$$

$$V_0 \equiv \sqrt{Re\phi} hv = \frac{V + \eta F}{\sqrt{2}} \quad (40c)$$

$$H_0 \equiv \phi \frac{\partial hv}{\partial \psi} = \frac{1}{\sqrt{2}} \frac{\partial V_0}{\partial \eta} \quad (40d)$$

$$G_0 \equiv \sqrt{Re} \phi^{3/2} \frac{\partial hv}{\partial \phi} = -\frac{1}{2} V_0 - \frac{\eta H_0}{\sqrt{2}} + \xi \frac{\partial V_0}{\partial \xi} \quad (40e)$$

The behavior of the basic-flow solution as $\psi \rightarrow \infty$ is also required. It follows from Eq. (36) that

$$U_0 \rightarrow 1 \quad (41a)$$

$$E_0 \rightarrow 0 \quad (41b)$$

Equation (32) can be rewritten as

$$\frac{\partial V}{\partial \eta} + 1 = (1 - F) + 2\xi \frac{\partial(1 - F)}{\partial \xi}$$

which upon integration with respect to η yields

$$V + \eta = \int_0^\eta (1 - F) d\eta + 2\xi \frac{\partial}{\partial \xi} \int_0^\eta (1 - F) d\eta$$

The integral in this equation is finite. As $\eta \rightarrow \infty$ it is proportional to the displacement thickness, hence

$$V + \eta \rightarrow \sqrt{2} g(\xi) \quad \text{as } \eta \rightarrow \infty$$

where $g(\xi)$ is a function of ξ . For the Falkner-Skan profiles, $g(\xi)$ becomes an absolute constant that depends on β_0 . For the Blasius flow this constant is 0.8604. Therefore,

$$V_0 \rightarrow g(\xi) \quad \text{as } \psi \rightarrow \infty \quad (41c)$$

$$H_0 \rightarrow 0 \quad \text{as } \psi \rightarrow \infty \quad (41d)$$

$$G_0 \rightarrow -\frac{1}{2} g(\xi) + \xi \frac{dg}{d\xi} \quad (41e)$$

It is worth noting that the transverse component of velocity V_0 and its streamwise derivative G_0 do not vanish outside the boundary layer. This is because the displacement thickness effect is neglected in the theory thus presented. However, we consider the flow due to the displacement thickness and its influence on the stability characteristics

only for the Blasius flow. Also, we note that the transverse component of the boundary-layer solution in the present coordinate system does not grow indefinitely as $\psi \rightarrow \infty$ for a non-zero pressure gradient. This is in contrast with the behavior of the v -component in the body-oriented axes where it grows linearly with y as $y \rightarrow \infty$. Therefore, we identify the present coordinate system as optimal to first order. Had we used the stream lines and potential lines of the inviscid flow over the displacement body we would have obtained optimal coordinates to second order^{18,19,20}. In such coordinates the behavior of the boundary-layer solution produces the inviscid outer flow to second order (i.e., it includes corrections due to displacement thickness).

E. Effect of the Displacement Thickness on the Blasius Flow

Van Dyke¹⁸ showed that the outer solution of the stream function ψ^0 for the second-order Blasius flow is

$$\psi^0 = y - \frac{\beta_1 \sqrt{2}}{\sqrt{Re}} \text{Real}(\sqrt{x + iy}) \quad (42)$$

and the inner solution is

$$\psi^i = \frac{\sqrt{2x}}{\sqrt{Re}} f_1\left(\frac{\sqrt{Re}}{\sqrt{2x}} y\right) + \frac{0}{Re} \quad (43)$$

where x and y are Cartesian coordinates (they are identical to ϕ and ψ for the case of a flat plate), $f_1(\eta)$ is the Blasius profile and $\beta_1 = 1.21678$. A second-order composite expansion can be formed from ψ^0 and ψ^i according to

$$\psi^c = \psi^i + \psi^0 - (\psi^i)^0$$

or

$$\psi^C = \frac{\sqrt{2x}}{\sqrt{Re}} \left\{ f_1 + \beta_1 [1 - \text{Real}(1 + i \frac{y}{x})^{1/2}] \right\} \quad (44)$$

Now, the v-component and its x-derivative defined by Eqs. (40c) and (40e) become

$$V_{02} = V_{01} - \frac{\beta_1}{\sqrt{2}} + \frac{\beta_1}{\sqrt{2}} \text{Real}(1 + i \frac{y}{x})^{-1/2} \quad (45)$$

and

$$G_{02} = G_{01} + \frac{\beta_1}{2\sqrt{2}} - \frac{\beta_1}{2\sqrt{2}} \text{Real} \left[\frac{1}{(1 + iy/x)^{3/2}} \right] \quad (46)$$

where V_{02} and G_{02} include displacement effects while V_{01} and G_{01} do not. We note that

$$V_{01} \rightarrow \beta_1/\sqrt{2} \quad \text{and} \quad G_{01} \rightarrow -\beta_1/2\sqrt{2}$$

as $y \rightarrow \infty$, and hence V_{02} and G_{02} vanish as $y \rightarrow \infty$, as they should.

III. The Disturbance Equations

We consider the stability of a basic flow over a two-dimensional curved wall with respect to three-dimensional disturbances in the form of alternating streamwise vortices, known as the Görtler vortices. However, we need not specify this type of disturbance at this stage of analysis. Instead we assume the total flow in the form

$$u = u_0(\phi, \psi) + u_1(\phi, \psi, z) \quad (47a)$$

$$v = v_0(\phi, \psi) + v_1(\phi, \psi, z) \quad (47b)$$

$$w = w_1(\phi, \psi, z) \quad (47c)$$

$$p = p_0(\phi, \psi) + p_1(\phi, \psi, z) \quad (47d)$$

where ϕ and ψ are the potential and stream functions of the inviscid basic flow and z is a rectilinear coordinate normal to the plane of the basic flow; u , v , and w are the velocity components in the ϕ , ψ , and z directions, respectively; and p is the static pressure. The subscript '0' denotes a basic-flow quantity while the subscript '1' denotes a perturbation quantity. Substituting these total flow quantities into the Navier-Stokes equations (see Appendix A), subtracting the basic-flow quantities, and keeping linear terms in the perturbation quantities, we obtain

ϕ -Momentum Equation

$$\begin{aligned} \frac{1}{\text{Re}} \nabla^2 u_1 - \tilde{v}_0 \frac{\partial u_1}{\partial \psi} - \tilde{u}_0 \frac{\partial u_1}{\partial \phi} + \left[-\frac{\partial \tilde{u}_0}{\partial \phi} + \frac{\tilde{u}_0}{h} \frac{\partial h}{\partial \phi} - \frac{\tilde{v}_0}{h} \frac{\partial h}{\partial \psi} - \frac{1}{\text{Re}} \frac{\nabla^2 h}{h} \right] u_1 \\ - \left(\frac{\partial \tilde{u}_0}{\partial \psi} - \frac{2\tilde{v}_0}{h} \frac{\partial h}{\partial \phi} \right) v_1 - \frac{2}{\text{Re}} \frac{1}{h} \frac{\partial h}{\partial \phi} \frac{\partial v_1}{\partial \psi} + \frac{2}{\text{Re}} \frac{1}{h} \frac{\partial h}{\partial \psi} \frac{\partial v_1}{\partial \phi} - h \frac{\partial p_1}{\partial \phi} = 0 \end{aligned} \quad (48)$$

ψ -Momentum Equation

$$\begin{aligned} \frac{1}{\text{Re}} \nabla^2 v_1 - \tilde{v}_0 \frac{\partial v_1}{\partial \psi} - \tilde{u}_0 \frac{\partial v_1}{\partial \phi} + \left[-\frac{\partial \tilde{v}_0}{\partial \psi} - \frac{\tilde{u}_0}{h} \frac{\partial h}{\partial \phi} + \frac{\tilde{v}_0}{h} \frac{\partial h}{\partial \psi} \right. \\ \left. - \frac{1}{\text{Re}} \frac{\nabla^2 h}{h} \right] v_1 - \left(\frac{\partial \tilde{v}_0}{\partial \phi} - \frac{2\tilde{u}_0}{h} \frac{\partial h}{\partial \psi} \right) u_1 + \frac{2}{\text{Re}} \frac{1}{h} \frac{\partial h}{\partial \phi} \frac{\partial u_1}{\partial \psi} \\ - \frac{2}{\text{Re}} \frac{1}{h} \frac{\partial h}{\partial \psi} \frac{\partial u_1}{\partial \phi} - h \frac{\partial p_1}{\partial \psi} = 0 \end{aligned} \quad (49)$$

z -Momentum Equation

$$\frac{1}{\text{Re}} \nabla^2 w_1 - v_0 \frac{\partial w_1}{\partial \psi} - \tilde{u}_0 \frac{\partial w_1}{\partial \phi} - h^2 \frac{\partial p_1}{\partial z} = 0 \quad (50)$$

Continuity Equation

$$\frac{\partial h u_1}{\partial \phi} + \frac{\partial h v_1}{\partial \psi} + h^2 \frac{\partial w_1}{\partial z} = 0 \quad (51)$$

where

$$\tilde{u}_0 = hu_0, \quad \tilde{v}_0 = hv_0, \quad (52)$$

$$\nabla^2 = \frac{\partial^2}{\partial \phi^2} + \frac{\partial^2}{\partial \psi^2} + h^2 \frac{\partial^2}{\partial z^2}, \quad (53)$$

$$Re = \rho^* U_\infty^* L^* / \mu^* \quad (54)$$

Equations (48) - (51) are the complete linearized form of the Navier-Stokes equations.

A. Scaled Variables

The disturbance equations, Eqs. (48) - (51), are non-dimensionalized with respect to an arbitrary length L^* . However, for stability analysis of boundary layers, the characteristic length should be based on a reference boundary-layer thickness. Hence we introduce the following scaled variables:

$$\overline{\phi} = \phi \quad (55a)$$

$$\overline{\psi} = \psi / \delta_0 \quad (55b)$$

$$\overline{z} = z / \delta_0 \quad (55c)$$

where

$$\delta_0 = \sqrt{\phi_0} / \sqrt{Re} \quad (56)$$

is a reference boundary-layer thickness evaluated at the streamwise location denoted by ϕ_0 . Also we define a Reynolds number based on δ_0 as

$$R = \delta_0 Re \quad (57)$$

In the new scaled variables, the disturbance equations, Eqs. (48) - (51), without any approximation become

φ-Momentum Equation

$$\begin{aligned} \delta_0^2 \frac{\partial^2 \bar{u}}{\partial \bar{\phi}^2} + \frac{\partial^2 \bar{u}}{\partial \bar{\psi}^2} + h^2 \frac{\partial^2 \bar{u}}{\partial \bar{z}^2} - m^{1/2} V_0 \frac{\partial \bar{u}}{\partial \bar{\psi}} - U_0 R \delta_0 \frac{\partial \bar{u}}{\partial \bar{\phi}} + (m H_0 - \frac{1}{2} m \beta_0 U_0 \\ + m^{1/2} V_0 h K_\psi - \delta_0^2 \frac{\nabla^2 h}{h}) \bar{u} - (m^{1/2} E_0 + \frac{m^{3/2}}{R^2} \beta_0 V_0) \bar{v} \\ + \frac{m}{R^2} \beta_0 \frac{\partial \bar{v}}{\partial \bar{\psi}} - \frac{2h}{R} \delta_0 K_\psi \frac{\partial \bar{v}}{\partial \bar{\phi}} - \frac{h}{R} \delta_0 \frac{\partial \bar{p}}{\partial \bar{\phi}} = 0 \end{aligned} \quad (58)$$

ψ-Momentum Equation

$$\begin{aligned} \delta_0^2 \frac{\partial^2 \bar{v}}{\partial \bar{\phi}^2} + \frac{\partial^2 \bar{v}}{\partial \bar{\psi}^2} + h^2 \frac{\partial^2 \bar{v}}{\partial \bar{z}^2} - m^{1/2} V_0 \frac{\partial \bar{v}}{\partial \bar{\psi}} - U_0 R \frac{\partial \bar{v}}{\partial \bar{\psi}} + (-m H_0 + \frac{1}{2} m \beta_0 U_0 \\ - m^{1/2} V_0 h K_\psi - \delta_0^2 \frac{\nabla^2 h}{h}) \bar{v} - (m^{3/2} G_0 + 2 U_0 R^2 h K_\psi) \bar{u} \\ - m^{3/2} \beta_0 \frac{\partial \bar{u}}{\partial \bar{\psi}} + 2 h K_\psi R \delta_0 \frac{\partial \bar{u}}{\partial \bar{\phi}} - h \frac{\partial \bar{p}}{\partial \bar{\psi}} = 0 \end{aligned} \quad (59)$$

z-Momentum Equation

$$\delta_0^2 \frac{\partial^2 \bar{w}}{\partial \bar{\phi}^2} + \frac{\partial^2 \bar{w}}{\partial \bar{\psi}^2} + h^2 \frac{\partial^2 \bar{w}}{\partial \bar{z}^2} - m^{1/2} V_0 \frac{\partial \bar{w}}{\partial \bar{\psi}} - U_0 R \delta_0 \frac{\partial \bar{w}}{\partial \bar{\phi}} - h^2 \frac{\partial \bar{p}}{\partial \bar{z}} = 0 \quad (60)$$

Continuity Equation

$$R \delta_0 \frac{\partial \bar{u}}{\partial \bar{\phi}} + \frac{\partial \bar{v}}{\partial \bar{\psi}} + h \frac{\partial \bar{w}}{\partial \bar{z}} - \frac{1}{2} \beta_0 m \bar{u} - h K_\psi \bar{v} = 0 \quad (61)$$

where

$$\bar{u} = u_1, \quad \bar{v} = R v_1, \quad \bar{w} = R w_1, \quad \bar{p} = R^2 p_1 \quad (62)$$

$$m = \phi_0 / \phi \quad (63)$$

$$K_\psi = \delta_0 k_\psi = - \frac{\delta_0}{h^2} \frac{\partial h}{\partial \psi} \quad (64)$$

$$\beta_0 = - \frac{2\phi}{h} \frac{\partial h}{\partial \phi} \quad (65)$$

and U_0 , V_0 , E_0 , H_0 , and G_0 are functions related to the basic flow through Eqs. (40a) - (40e).

We identify β_0 with the pressure gradient parameter defined by Eq. (33) and k_ψ as the curvature of the inviscid streamlines. The value of k_ψ at $\psi = 0$ is the curvature of the wall. In general, k_ψ is a function of ϕ and ψ .

B. A Normal Mode Solution

Equations (58) - (61) constitute a system of homogeneous linear partial-differential equations with variable coefficients. They are of the elliptic type. The class of disturbances considered here is the Görtler vortices. That is, the disturbances are periodic in the z -direction. The dependence on \bar{z} can be eliminated from the disturbance equations once the wavelength of the periodic disturbances is specified. The result is a system of partial-differential equations in $\bar{\phi}$ and $\bar{\psi}$ as independent variables. Now, the boundary conditions are

$$\bar{u} = \bar{v} = \bar{w} = 0 \quad \text{at} \quad \bar{\psi} = 0 \quad (66)$$

$$\bar{u}, \bar{v}, \text{ and } \bar{w} \rightarrow 0 \quad \text{as} \quad \bar{\psi} \rightarrow \infty \quad (67)$$

Conditions (66) are the no-slip and no-penetration conditions for solid walls. Conditions (67) express the physical fact that the disturbances must decay in the free stream. For high Reynolds numbers, the basic-flow quantities are slowly varying with $\bar{\phi}$. Consequently, the basic flow can be considered quasi-parallel, thereby allowing the separation of $\bar{\phi}$ from the disturbance equations. Hence, we evaluate the basic-flow variables at a fixed location, say ϕ_0 , and assume the solution in the normal-mode form

$$\bar{u} = u(\bar{\psi}) \cos \alpha \bar{z} e^{\sqrt{\sigma} d \bar{\phi}} \quad (68a)$$

$$\bar{v} = v(\bar{\psi}) \cos \alpha \bar{z} e^{\sqrt{\sigma} d \bar{\phi}} \quad (68b)$$

$$\bar{w} = w(\bar{\psi}) \sin \alpha \bar{z} e^{\sqrt{\sigma} d \bar{\phi}} \quad (68c)$$

$$\bar{p} = p(\bar{\psi}) \cos \alpha \bar{z} e^{\sqrt{\sigma} d \bar{\phi}} \quad (68d)$$

The functions u , v , w , and p on the right-hand side should not be confused with the total flow variables defined in Eqs. (47a) - (47d), which will not be referenced in the rest of this paper. Substituting Eqs. (68a) - (68d) into Eqs. (58) - (61), we obtain

ϕ -Momentum Equation

$$u'' - V_0 u' + (H_0 - h^2 \alpha^2 - \sigma U_0 - \frac{1}{2} \beta_0 U_0) u - E_0 v + \Gamma_1 = 0 \quad (69)$$

ψ -Momentum Equation

$$\begin{aligned} v'' - V_0 v' + (-H_0 - h^2 \alpha^2 - \sigma U_0 + \frac{1}{2} \beta_0 U_0) v - (2U_0 h G_N^2 + G_0) u \\ - \beta_0 u' - h p' + \Gamma_2 = 0 \end{aligned} \quad (70)$$

z -Momentum Equation

$$w'' - V_0 w' + (-h^2 \alpha^2 - \sigma U_0) w + h^2 \alpha p + \Gamma_3 = 0 \quad (71)$$

Continuity Equation

$$v' + (\sigma - \frac{1}{2} \beta_0) u + h \alpha w + \Gamma_4 = 0 \quad (72)$$

where

$$\sigma = R \bar{\sigma} \quad (73)$$

$$\begin{aligned} \Gamma_1 = (V_0 h K_\psi + \frac{\delta_\sigma}{R} \frac{d\sigma}{d\bar{\phi}} + \frac{\sigma^2}{R^2} - \frac{\delta_\sigma^2 \nabla^2 h}{h}) u - \frac{1}{R^2} (\beta_0 V_0 + 2h K_\psi \sigma) v + \frac{\beta_0}{R^2} v' \\ - \frac{h\sigma}{R^2} p \end{aligned} \quad (74)$$

$$\Gamma_2 = (-V_0 h K_\psi + \frac{\delta_0}{R} \frac{d\sigma}{d\bar{\phi}} + \frac{\sigma^2}{R^2} - \delta_0^2 \frac{\nabla^2 h}{h})v + 2h K_\psi \sigma u \quad (75)$$

$$\Gamma_3 = (\frac{\delta_0}{R} \frac{d\sigma}{d\bar{\phi}} + \frac{\sigma^2}{R^2})w \quad (76)$$

$$\Gamma_4 = -h K_\psi v \quad (77)$$

$$G_N^2 = R^2 K_\psi \quad (78)$$

and prime denotes differentiation with respect to $\bar{\psi}$.

The variation of the streamline curvature in the ψ -direction (i.e., normal to the wall) is included in the function K_ψ . Hence, in general, G_N^2 is a function of $\bar{\psi}$. We identify the value of G_N at $\bar{\psi} = 0$ as the Görtler Number. Recalling the definitions of R and K_ψ , Eqs. (57) and (64), we see that the present definition of Görtler number is based on the reference boundary-layer thickness δ_0 , while the original parameter identified by Görtler is based on the momentum thickness. However, the two thicknesses are related (e.g., for the Blasius profile $\delta_m = 0.664 \delta_0$).

The boundary conditions, Eqs. (66) and (67), become

$$u = v = w = 0 \quad \text{at} \quad \bar{\psi} = 0 \quad (79)$$

$$u, v, \text{ and } w \rightarrow 0 \quad \text{as} \quad \bar{\psi} \rightarrow \infty \quad (80)$$

The homogeneous system defined by Eqs. (69) - (72), (79), and (80) is an eigenvalue problem. The characteristic equation of this eigenvalue problem may have the form

$$\Gamma(\alpha, \sigma, R) = 0 \quad (81)$$

where α is the wavenumber, σ is the growth (amplification) rate, and R is a reference Reynolds number. Because of the dependence of the basic flow on the wall geometry and the explicit existence of the metric

coefficient h and its derivatives in Eqs. (69) - (72), the surface given by Eq. (81) is configuration dependent. That is, in general, each geometry may have different characteristic surfaces in the space α , σ , and R .

C. An Equivalent System of First-Order Equations

Equations (69) - (72) are reduced to a system of first-order differential equations by letting

$$z_1 = u, \quad z_2 = u', \quad z_3 = v, \quad z_4 = w, \quad z_5 = w' \quad \text{and} \quad z_6 = hp$$

The result is

$$z' = Az \tag{82}$$

where z is the vector

$$z = \{z_1, z_2, z_3, z_4, z_5, z_6\}^T \tag{83}$$

and A is a matrix that can be written as the sum of two matrices according to

$$A = A_0 + \Delta A \tag{84}$$

$$A_0 = \begin{bmatrix} 0 & 1 & 0 & 0 & 0 & 0 \\ \alpha^2 + \sigma U_0 - H_0 + \frac{1}{2} \beta_0 U_0 & V_0 & E_0 & 0 & 0 & 0 \\ -\sigma + \frac{1}{2} \beta_0 & 0 & 0 & -\alpha & 0 & 0 \\ 0 & 0 & 0 & 0 & 1 & 0 \\ 0 & 0 & 0 & \alpha^2 + \sigma U_0 & V_0 & -\alpha \\ -\Lambda & -\sigma - \frac{1}{2} \beta_0 & -(\alpha^2 + \sigma U_0 + H_0 - \frac{1}{2} \beta_0 U_0) & \alpha V_0 & -\alpha & 0 \end{bmatrix}$$

where

$$\Lambda = 2U_0 G_N^2 - \sigma V_0 + G_0 + \frac{1}{2} \beta_0 V_0 \tag{85}$$

and the matrix ΔA is given in Appendix C. We note that the matrix A_0 contains all the terms of $O(1)$, while the matrix ΔA contains all the higher-order terms. The boundary conditions for the system (82) are

$$z_1 = z_3 = z_4 = 0 \quad \text{at} \quad \bar{\psi} = 0 \quad (86)$$

$$z_1, z_3, \text{ and } z_4 \rightarrow 0 \quad \text{as} \quad \bar{\psi} \rightarrow \infty \quad (87)$$

We recall the fact that the Görtler number G_N in Eq. (85) is a function of $\bar{\psi}$.

The above reduction of the governing equations to a system of six first-order equations requires the first derivatives of the basic-flow quantities. In the work of Smith¹² and Floryan and Saric¹³, the disturbance equations were reduced to two coupled equations, one of second order in the u -component and the other of fourth order in the v -component. Then, Floryan and Saric reduced the new equations to a system of six first-order equations. However, their method requires some of the second-order derivatives of the basic flow, which demands a higher accuracy of the basic-flow solution than it is required in the present method.

We define a basic system as

$$z' = A_0 z \quad (88)$$

subject to the boundary conditions (86) and (87). We note that the zeroth-order disturbance equations developed by Floryan and Saric¹³ for the case of a circular arc can be put in the form (88). A method for solving the basic system is presented in Section IV. However, the eigenvalues of the basic system will be slightly different from those of the original system, Eqs. (82), because the matrix ΔA was not included. In Section V, a perturbation procedure is presented to obtain the

correction to the eigenvalues due to a small deviation of the coefficient matrix from a basic value.

IV. A Method For Solving The Basic System

The system (88) subject to boundary conditions (86) and (87) is a two-point boundary-value problem. As mentioned previously, this is an eigenvalue problem. Any one of the parameters α , σ , and R can be treated as the eigenvalue when the other two parameters are prescribed. An alternative to the parameter R is the Görtler number $G_N(0)$ based on the wall curvature, in which case we rewrite Eq. (85) as

$$\Lambda = 2U_0 G_N^2(0) r(\bar{\psi}) - \sigma V_0 + G_0 + \frac{1}{2} B_0 V_0 \quad (89)$$

where $r(0) = 1$. If the deviation of the curvature of the streamlines from the value at the wall is neglected, then $r \equiv 1$ for all $\bar{\psi}$ and $G_N(0)$ is the eigenvalue. However, for the purpose of the present section, r is assumed to be

$$\begin{aligned} r &= r(\bar{\psi}) & \text{for } 0 \leq \bar{\psi} \leq \bar{\psi}_m \\ r &= r(\bar{\psi}_m) & \bar{\psi} > \bar{\psi}_m \end{aligned} \quad (90)$$

The difference between $r(\bar{\psi})$ and $r(\bar{\psi}_m)$ for $\bar{\psi} > \bar{\psi}_m$ will be accounted for by the perturbation technique presented in Section V.

A. Boundary Conditions at Infinity

Application of the asymptotic boundary condition (87) at a finite value of $\bar{\psi}$ may lead to inaccurate results. However, outside the boundary layer (i.e., $\bar{\psi} > 10$), the system of equations has constant coefficients because

$$U_0 \rightarrow 1, \quad H_0 \rightarrow 0, \quad V_0 \rightarrow \bar{V}_0, \quad E_0 \rightarrow 0,$$

$$\text{and } G_0 \rightarrow \bar{G}_0 \quad \text{as } \bar{\psi} \rightarrow \infty,$$

where \bar{V}_0 and \bar{G}_0 are constants. Thus, we write the system of constant coefficients as

$$z' = Cz \tag{91}$$

where

$$C = \begin{bmatrix} 0 & 0 & 0 & 0 & 0 & 0 \\ \alpha^2 + \sigma + \frac{1}{2} \beta_0 & \bar{V}_0 & 0 & 0 & 0 & 0 \\ -\sigma & 0 & 0 & -\alpha & 0 & 0 \\ 0 & 0 & 0 & 0 & 1 & 0 \\ 0 & 0 & 0 & \alpha^2 + \sigma & \bar{V}_0 & -\alpha \\ -\bar{\Lambda} & -\sigma - \frac{1}{2} \beta_0 & -(\alpha^2 + \sigma - \frac{1}{2} \beta_0) & \alpha & -\alpha & 0 \end{bmatrix} \tag{92}$$

and

$$\bar{\Lambda} = 2G_N^2(0)r(\bar{\psi}_m) - \sigma\bar{V}_0 + G_0 + \frac{1}{2} \beta_0 \bar{V}_0 \tag{93}$$

Let us denote the characteristic roots of C by $\lambda_1, \lambda_2, \dots, \lambda_6$ where the λ_n are given by

$$\lambda^2 - \bar{V}_0 \lambda - (\alpha^2 + \sigma + \frac{1}{2} \beta_0) = 0 \tag{94a}$$

$$\lambda^4 - \bar{V}_0 \lambda^3 - (2\alpha^2 + \sigma) \lambda^2 + \alpha^2 \bar{V}_0 \lambda + \alpha^2 (\alpha^2 + \sigma - \frac{1}{2} \beta_0) = 0 \tag{94b}$$

We consider the case in which three of the λ_n are positive real numbers, while the other three are negative real numbers. Let λ_1, λ_2 , and λ_3 be the positive roots. When $\beta_0 = 0$, the characteristic roots of C reduce to

$$\alpha, \lambda_2, \lambda_3, -\alpha, \lambda_5, \text{ and } \lambda_6 \tag{95}$$

where

$$\lambda_2 = \lambda_3 = \frac{1}{2} [V_0 + \sqrt{V_0^2 + 4(\alpha^2 + \sigma)}] \quad (96a)$$

and

$$\lambda_5 = \lambda_6 = -\frac{1}{2} [-V_0 + \sqrt{V_0^2 + 4(\alpha^2 + \sigma)}] \quad (96b)$$

For the special case $\sigma = \alpha V_0$, Eq. (96b) gives

$$\lambda_5 = \lambda_6 = -\alpha$$

so that $-\alpha$ is a root of multiplicity 3. When $\sigma < -\frac{1}{4}(V_0^2 + 4\alpha^2)$ Eqs. (96) show that $\lambda_2, \lambda_3, \lambda_5$, and λ_6 are complex. This case of complex roots is not treated in the present work as mentioned earlier.

Now, an analytic solution to the system (91) is easily obtained in terms of elementary functions. The system (89) has six linearly independent solutions. The general solution is obtained by superposition of these fundamental solutions. Hence, we write

$$z = Yb \quad (97)$$

where the i th component of the vector b is

$$b_i = c_i \exp(\lambda_i \bar{\psi}) \quad (98)$$

The fundamental matrix Y is not a constant matrix in the case of repeated roots. It includes linear terms in $\bar{\psi}$ when $\beta_0 = 0$; for the special case when $-\alpha$ has a multiplicity of 3, it includes quadratic terms in $\bar{\psi}$. Therefore, its value depends on $\bar{\psi}$.

Because of the linear independence of the fundamental solutions, the system (97) can be inverted to yield

$$Y^{-1}z = b \quad (99)$$

Now the asymptotic boundary condition (87) requires that $b_1 = b_2 = b_3 = 0$, as can be seen from Eq. (97) and (98). It follows from Eq. (99) that

$$Tz = \{0\} \quad (100)$$

where T is a 3×6 rectangular matrix given by

$$T_{i,j} = [Y^{-1}]_{ij} \quad \begin{matrix} i = 1, 2, 3 \\ j = 1, \dots, 6 \end{matrix} \quad (101)$$

where $[Y^{-1}]_{ij}$ denotes the element ij of the matrix Y^{-1} .

By evaluating T at a finite value of $\bar{\psi} = \bar{\psi}_m$, Eq. (100) provides three boundary conditions in the form of linear combinations of the values of the variables z_1, \dots, z_6 at $\bar{\psi} = \bar{\psi}_m$. This form suits the method used to integrate the basic system for $\bar{\psi} \leq \bar{\psi}_m$.

We note that the matrix T in Eqs. (100) depends on $\bar{\psi}_m$ when $\beta_0 = 0$, which is calculated by inverting a 6×6 matrix for each iteration and for each eigenvalue. Next, we develop an alternative form for T that is independent of $\bar{\psi}$. To accomplish this, we reduce the matrix C to a Jordan canonical form by introducing the similarity transformation

$$J = P^{-1}CP \quad (102)$$

When $\beta_0 \neq 0$, the λ_n are distinct and their corresponding eigenvectors are orthogonal. In this case, J is a diagonal matrix and P is a matrix whose columns are the eigenvectors of C . We arrange these columns so that the positive eigenvalues appear in the first three rows. When $\beta_0 = 0$, $\lambda_2 = \lambda_3$ and $\lambda_5 = \lambda_6$, and hence J has the form

$$J = \begin{bmatrix} \alpha & 0 & 0 & 0 & 0 & 0 \\ 0 & \lambda_2 & \tau_1 & 0 & 0 & 0 \\ 0 & 0 & \lambda_2 & 0 & 0 & 0 \\ 0 & 0 & 0 & -\alpha & 0 & 0 \\ 0 & 0 & 0 & 0 & \lambda_5 & \tau_2 \\ 0 & 0 & 0 & 0 & 0 & \lambda_5 \end{bmatrix} \quad (103)$$

where τ_1 and τ_2 are constants that we do not need to specify. In this case, P is defined in Appendix D. Letting

$$z = P\xi \quad (104)$$

in (91) and using (102), we obtain

$$\xi' = J\xi \quad (105)$$

We note that the characteristic roots in J are arranged such that the first three roots are the positive roots. Therefore, for decaying solutions as $\bar{\psi} \rightarrow \infty$, we must impose the conditions

$$\xi_1 = \xi_2 = \xi_3 = 0 \quad (106)$$

Since $\xi = P^{-1}z$ according to Eq. (104), conditions (106) yield

$$Tz = \{0\} \quad (107)$$

where T consists of the first three rows of P^{-1} .

Although the matrix T of Eq. (107) does not depend on $\bar{\psi}$, it is calculated by inverting the 6×6 matrix P for each iteration and for each eigenvalue. Next, we use the concept of adjoint to develop a matrix T that does not require inversion of a matrix. To accomplish this, we multiply Eq. (88) with $z^{*T}(\bar{\psi})$, integrate the result by parts from $\bar{\psi} = 0$ to $\bar{\psi} = \bar{\psi}_m$, and obtain²¹

$$z^{*T}z \Big|_0^{\bar{\psi}_m} - \int_0^{\bar{\psi}_m} \left(\frac{dz^{*T}}{d\bar{\psi}} + z^{*T}A_0 \right) z d\bar{\psi} = 0 \quad (108)$$

The equations defining the adjoint z^* are obtained by setting the coefficient of z in the integrand in Eq. (108) equal to zero. The result is

$$\frac{dz^{*T}}{d\bar{\psi}} + z^{*T}A_0 = 0$$

which upon transposition becomes

$$\frac{dz^*}{d\bar{\psi}} + A_0^T z^* = 0 \quad (109)$$

Then, Eq. (108) becomes

$$z^{*T} z \Big|_{\bar{\psi}_m} - z^{*T} z \Big|_0 = 0 \quad (110)$$

We recall that the boundary conditions at $\bar{\psi} = 0$ are defined in Eq. (86), while the boundary conditions at $\bar{\psi}_m$ are defined in Eq. (107), where T consists of the first three rows of P^{-1} . We choose the adjoint boundary conditions such that the two terms in Eq. (110) vanish independently; that is

$$z^{*T} z = 0 \quad \text{at} \quad \bar{\psi} = \bar{\psi}_m \quad (111)$$

$$z^{*T} z = 0 \quad \text{at} \quad \bar{\psi} = 0 \quad (112)$$

In expanded form, Eq. (112) becomes

$$z_1^* z_1 + z_2^* z_2 + z_3^* z_3 + z_4^* z_4 + z_5^* z_5 + z_6^* z_6 = 0 \quad \text{at} \quad \bar{\psi} = 0$$

which upon using Eq. (86) reduces to

$$z_2^* z_2 + z_5^* z_5 + z_6^* z_6 = 0 \quad \text{at} \quad \bar{\psi} = 0 \quad (113)$$

We choose the boundary conditions at $\bar{\psi} = 0$ such that each of the coefficients of $z_2(0)$, $z_5(0)$, and $z_6(0)$ vanish independently. The result is

$$z_2^* = z_5^* = z_6^* = 0 \quad \text{at} \quad \bar{\psi} = 0 \quad (114)$$

To define the boundary conditions at $\bar{\psi} = \bar{\psi}_m$, we view Eq. (104) as a linear transformation relating ξ and z at $\bar{\psi} = \bar{\psi}_m$. Substituting Eq. (104) into (111), we have

$$z^{*T} P \xi = 0 \quad \text{at} \quad \bar{\psi} = \bar{\psi}_m$$

or

$$(P^T z^*)^T \xi = 0 \quad \text{at} \quad \bar{\psi} = \bar{\psi}_m \quad (115)$$

Letting

$$\xi^* = P^T z^* \quad (116)$$

we rewrite Eq. (115) as

$$\xi^{*T} \xi = 0 \quad \text{at} \quad \bar{\psi} = \bar{\psi}_m \quad (117)$$

or

$$\xi_1^* \xi_1 + \xi_2^* \xi_2 + \xi_3^* \xi_3 + \xi_4^* \xi_4 + \xi_5^* \xi_5 + \xi_6^* \xi_6 = 0 \quad \text{at} \quad \bar{\psi} = \bar{\psi}_m \quad (118)$$

Using the boundary conditions (106), which are equivalent to the boundary conditions (107), we reduce Eq. (118) to

$$\xi_4^* \xi_4 + \xi_5^* \xi_5 + \xi_6^* \xi_6 = 0 \quad \text{at} \quad \bar{\psi} = \bar{\psi}_m \quad (119)$$

Since ξ_4 , ξ_5 , and ξ_6 are linearly independent because P is a nonsingular matrix, each of their coefficients must vanish independently; that is

$$\xi_4^* = \xi_5^* = \xi_6^* = 0 \quad \text{at} \quad \bar{\psi} = \bar{\psi}_m \quad (120)$$

Then, it follows from Eq. (116) and (120) that the adjoint boundary conditions at $\bar{\psi} = \bar{\psi}_m$ are

$$T^* z^* = 0 \quad \text{at} \quad \bar{\psi} = \bar{\psi}_m \quad (121)$$

where T^* consists of the last three rows of P^T when $\beta_0 = 0$ and Y^T when $\beta_0 \neq 0$. We note that the calculation of T^* does not involve any matrix inversion. Thus, the adjoint problem is defined by Eq. (109) subject to the boundary conditions (114) and (121).

To determine boundary conditions for z that do not involve inversion of matrices, we consider the adjoint of the adjoint problem. When $\bar{\psi} > \bar{\psi}_m$, Eq. (109) becomes

$$\frac{dz^*}{d\bar{\psi}} + C^T z^* = 0 \quad (122)$$

As before, we reduce the matrix $C^* = -C^T$ into a Jordan canonical form by using the similarity transformation

$$J^* = P^{*-1} C^* P^* \quad (123)$$

When $\beta_0 \neq 0$, the λ_n are distinct and their corresponding eigenvectors are orthogonal. In this case, J^* is a diagonal matrix and P^* is a matrix whose columns are the eigenvectors of C^* . We arrange these columns so that the positive eigenvalues appear in the first three rows. When $\beta_0 = 0$, J^* has the form

$$J^* = \begin{bmatrix} \alpha & 0 & 0 & 0 & 0 & 0 \\ 0 & \lambda_2^* & \tau_1^* & 0 & 0 & 0 \\ 0 & 0 & \lambda_2^* & 0 & 0 & 0 \\ 0 & 0 & 0 & -\alpha & 0 & 0 \\ 0 & 0 & 0 & 0 & \lambda_5^* & \tau_2^* \\ 0 & 0 & 0 & 0 & 0 & \lambda_5^* \end{bmatrix} \quad (124)$$

where τ_1^* and τ_2^* are constants and $\lambda_2^* = -\lambda_5$ and $\lambda_5^* = -\lambda_2$. In this case, P^* is defined in Appendix D. Then, using the transformation

$$z^* = P^* \xi^* \quad (125)$$

we rewrite (122) as

$$\frac{d\xi^*}{d\bar{\psi}} = J^* \xi^* \quad (126)$$

Hence, for decaying solutions, we must put

$$\xi_1^* = \xi_2^* = \xi_3^* = 0 \quad \text{at} \quad \bar{\psi} = \bar{\psi}_m \quad (127)$$

Then, following steps similar to those in Eq. (108) - (121), we find that the boundary conditions for z at $\bar{\psi} = \bar{\psi}_m$ are

$$Tz = 0 \quad \text{at} \quad \bar{\psi} = \bar{\psi}_m \quad (128)$$

where T consists of the last three rows of P^{*T} , which do not involve inversion of matrices.

B. Boundary Conditions at the Wall

The boundary conditions (86) and (114) can be rewritten in matrix form as

$$Wz = \{0\} \quad \text{at} \quad \bar{\psi} = 0 \quad (129)$$

for the basic system, and

$$W^* z^* = \{0\} \quad \text{at} \quad \bar{\psi} = 0 \quad (130)$$

for the adjoint system. Here, W and W^* are 3×6 rectangular matrices with all elements being zero except that

$$W_{11} = W_{23} = W_{34} = W_{12}^* = W_{25}^* = W_{36}^* = 1$$

In summary, the basic system is defined by Eqs. (88), (128), and (129), and the adjoint system is defined by Eqs. (109), (121), and (130).

C. Numerical Procedure

Numerical integration of these two-point boundary-value problems are obtained by using a computer code (SUPPORT) developed by Scott and Watts²². The method of integration uses superposition coupled with an orthonormalization procedure and a variable-step Runge-Kutta-Fehlberg scheme. We fix the values of any two of the parameter α , σ , and G_N , and consider the third one as an eigenvalue. We make an initial guess for

the eigenvalue. Starting at the position $\bar{\psi} = \bar{\psi}_m$, we carry out the integration toward the wall $\bar{\psi} = 0$. One of the boundary conditions at the wall will not be satisfied if the guessed eigenvalue is not the exact value. A Newton-Raphson iteration process is used to obtain a better approximation of the eigenvalue. The computer code is designed such that the boundary condition that has to be iterated on is the last specified one. Hence, for the basic system we iterate on the condition $z_4 = 0$ at the wall. The condition of convergence was taken as

$$|z_4(0)/\hat{z}_4| < 10^{-6} \quad (131)$$

where \hat{z}_4 is the maximum value of z_4 in the domain of numerical integration. For the adjoint problem the condition was taken as

$$|z_6^*(0)/\hat{z}_6^*| < 10^{-6} \quad (132)$$

Conditions (131) and (132) were used for all the calculations presented in this paper. However, for some of the cases, higher accuracy was used in Eqs. (131) and (132). However, the change in the eigenvalues and eigenfunctions are of $O(10^{-6})$.

V. A Perturbation Procedure to Account for Small Deviations in the Matrix A_0

The matrix A in Eq. (84) is expressed as the sum of two matrices A_0 and ΔA , where the elements of ΔA are small compared with those of A_0 . In Section IV we presented a method of solution for the basic system whose matrix is A_0 . Now, we present a perturbation approach to find the change in the eigenvalue due to a small change A_1 in A_0 . However, we need not identify the change A_1 as the matrix ΔA in Eq. (84). The matrix A_1 represents a general, however, small change in A_0 ; A_1 may incorporate, in addition to ΔA , changes in the basic-flow quantities due

to displacement speed and/or viscous curvature effects. Since the perturbation in the eigenvalue due to each higher-order effect is small, then interaction between these effects is negligible. Hence, one may study the influence of each higher-order term independent of the others. This will point out which second-order terms are the most stabilizing or destabilizing. This is helpful in the aerodynamic design of surfaces with regions of concave curvature.

We consider the eigenvalue problem

$$z' = (A_0 + \epsilon A_1)z \quad (133)$$

with the boundary conditions (86) and (87). We assume that $\epsilon \ll 1$.

First we solve the basic system

$$z_0' = A_0 z_0 \quad (134)$$

with the same boundary conditions. Let λ_0 denote the eigenvalue of this system. We expand the solution for system (133) in the form

$$z = z_0 + \epsilon \zeta \quad (135)$$

and the eigenvalue as

$$\lambda = \lambda_0 + \epsilon \lambda_1 \quad (136)$$

Since A_0 depends on the eigenvalue λ , we use the Taylor-series expansion

$$A_0(\lambda_0 + \epsilon \lambda_1) = A_0(\lambda_0) + \left. \frac{\partial A_0}{\partial \lambda} \right|_{\lambda_0} \epsilon \lambda_1 + \dots \quad (137)$$

Substituting expansions (135) and (137) into Eq. (133), neglecting terms $O(\epsilon^2)$, and using Eq. (134), we obtain

$$\zeta' - A_0 \zeta = \left(\lambda_1 \left. \frac{\partial A_0}{\partial \lambda} \right|_{\lambda_0} + A_1 \right) z_0 \quad (138)$$

The boundary conditions (86) and (87) give

$$\zeta_1 = \zeta_3 = \zeta_4 = 0 \quad \text{at} \quad \bar{\psi} = 0 \quad (139)$$

$$\zeta_1, \zeta_3, \zeta_4 \rightarrow 0 \quad \text{as} \quad \bar{\psi} \rightarrow \infty \quad (140)$$

Since the homogeneous problem obtained from the system (138) - (140) has a nontrivial solution, namely z_0 , then the nonhomogeneous problem has a solution if and only if a solvability condition is satisfied²¹. To obtain this condition, we multiply Eq. (138) by the solution z_0^{*T} of the adjoint homogeneous problem and integrate the result from $\bar{\psi} = 0$ to $\bar{\psi} \rightarrow \infty$. The result is

$$\lambda_1 = - \frac{\int_0^\infty z_0^{*T} A_1 z_0 d\bar{\psi}}{\int_0^\infty z_0^{*T} \frac{\partial A_0}{\partial \lambda} \bigg|_{\lambda_0} z_0 d\bar{\psi}} \quad (141)$$

Hence, the eigenvalue of the original system (133) becomes

$$\lambda = \lambda_0 - \frac{\int_0^\infty z_0^{*T} \epsilon A_1 z_0 d\bar{\psi}}{\int_0^\infty z_0^{*T} \frac{\partial A_0}{\partial \lambda} \bigg|_{\lambda_0} z_0 d\bar{\psi}} \quad (142)$$

The integrals in Eq. (142) have to be evaluated numerically. In the interval $0 \leq \bar{\psi} \leq \bar{\psi}_m$ the values of z_0 and z_0^* are known from the numerical solution of the basic problem and its adjoint. For $\bar{\psi} > \bar{\psi}_m$ the analytic solution outside the boundary layer is used. The eigenvalue λ in Eq. (142) can be identified as α , σ , or R and its alternative $G_N^2(0)$. However, from the structure of the matrix A_0 , it is advantageous to identify λ with $G_N^2(0)$ since in this case all elements in the matrix $\partial A_0 / \partial \lambda$ are zero except one element. Let D_{ij} denote an element

of $\partial A_0 / \partial \lambda$, hence $D_{ij} = 0$ for all i and j except

$$D_{61} = -2U_0 r \quad (143)$$

where r is defined by Eq. (90). Thus, Eq. (142) gives

$$\lambda = \lambda_0 + \frac{\int_0^\infty z_0^* \epsilon A_1 z_0 d\bar{\psi}}{2 \int_0^\infty r U_0 z_6^* z_1 d\bar{\psi}} \quad (144)$$

where z_1 is the first component of z_0 and z_6^* is the sixth component of z_0^* . In Eq. (144), λ and λ_0 stand for $G_N^2(0)$ with and without the correction due ϵA_1 , respectively.

As a first application, we consider the correction due to restricting the function $r(\bar{\psi})$ to be a constant for $\bar{\psi} > \bar{\psi}_m$. Let B_{ij} denote an element of ϵA_1 , then $B_{ij} = 0$ for all i and j except

$$B_{61} = \begin{cases} 0 & \text{for } \bar{\psi} \leq \bar{\psi}_m \\ 2U_0 \lambda_0 [r(\bar{\psi}_m) - r(\bar{\psi})] & \text{for } \bar{\psi} > \bar{\psi}_m \end{cases} \quad (145)$$

We note that $U_0 = 1$ for $\bar{\psi} > \bar{\psi}_m$. Equation (144) gives

$$\lambda / \lambda_0 = (I_1 + I_3) / (I_1 + I_2) \quad (146)$$

where

$$I_1 = \int_0^{\bar{\psi}_m} r U_0 z_6^* z_1 d\bar{\psi} \quad (147a)$$

$$I_2 = \int_{\bar{\psi}_m}^\infty r z_6^* z_1 d\bar{\psi} \quad (147b)$$

$$I_3 = r(\bar{\psi}_m) \int_{\bar{\psi}_m}^\infty z_6^* z_1 d\bar{\psi} \quad (147c)$$

As a second application of Eq. (144), we consider the effect of displacement thickness of the Blasius flow. It follows from Eqs. (45) and (46) that the perturbations in V_0 and G_0 are

$$V_1 = -\bar{V}_0[1 - \text{Real}(t^{1/2})] \quad (148)$$

$$G_1 = \frac{1}{2} \bar{V}_0[1 - \text{Real}(t^{3/2})] \quad (149)$$

where

$$t = (1 + i\bar{\psi}/\sqrt{\text{Re}\phi_0})^{-1} \quad (150)$$

The nonzero elements of ϵA_1 are $B_{22} = V_1$, $B_{55} = V_1$, $B_{61} = \sigma V_1 - G_1$, and $B_{64} = \alpha V_1$. Then Eq. (144) gives

$$\begin{aligned} \lambda = \lambda_0 + \int_0^\infty [V_1(z_2 z_2^* + z_5 z_5^* + \alpha z_4 z_6^* + \sigma z_1 z_6^* \\ - G_1 z_1 z_6^*) d\bar{\psi} / \int_0^\infty 2U_0 z_1 z_6^* d\bar{\psi} \end{aligned} \quad (151)$$

The destabilizing effect of G_1 is clear from Eq. (151) since its contribution to the integral is negative.

VI. Results and Discussion

Görtler¹ showed that the centrifugal instability of boundary-layer flows along concavely curved walls is primarily a function of the momentum thickness of the basic-flow profile and not of the details of the shape of the boundary layer. We recall that in Görtler's model the transverse component of the basic flow was neglected. This component was accounted for in the models of Smith¹² and Floryan and Saric¹³. Very accurate numerical calculations of the neutral stability curves of these two models for the Blasius profile were provided by Floryan and Saric¹³.

Their results demonstrated the destabilizing effect of the transverse component of the basic flow, especially for small wavenumbers.

A. The Blasius Flow

Figure 4 shows the neutral stability curves for the Blasius flow obtained for different models. Curve 1 in Fig. 4 is Görtler's model. The pertinent equations are obtained from the basic system, Eq. (88), by setting $V_0 = G_0 = H_0 = 0$ for all $\bar{\psi}$ (i.e., we neglect the terms due to the transverse component of the basic flow). Curve 2 is the present model, Curve 3 is the Floryan-Saric¹³ model, and Curve 4 is a modified Smith model. The governing equations of these three models are identical, Eq. (88). The differences among the neutral stability curves of these models, as shown in Fig. 4, are due to different treatments of the term G_0 . In the present model, Curve 2, $G_0 \rightarrow -1/2 V_0 = -0.4302$ as $\bar{\psi} \rightarrow \infty$, as can be seen from Eq. (41e). Outside the boundary layer (i.e., $\bar{u} \approx 1.0$), the terms V_0 and G_0 represent the slope and curvature of the viscous streamlines, respectively. As discussed in Section II, these terms do not vanish outside the boundary layer in both the first- and second-order boundary-layer solutions. However, as $\eta \rightarrow \infty$ they vanish only in the second-order solution when we account for the displacement-thickness effect. Floryan and Saric¹³, in the calculation of Curve 3, put $\partial V_0 / \partial \phi_1 = 0$ for $\bar{\psi} \geq \bar{\psi}_m$, where $\phi_1 = \epsilon_V \phi$ and $\epsilon_V = 1/R$. Equation (39e) shows that the part that does not vanish as $\eta \rightarrow \infty$ in the expression of $\partial h v / \partial \phi$ is the first term, namely $(V + \eta F)$. When we neglected this term everywhere (i.e., for all $\bar{\psi}$), we obtained a neutral stability curve that is indistinguishable from Curve 3 of Floryan and Saric. We recall that in the Smith¹² model, the term $\partial h v / \partial \phi$ was not

included in the analysis. Hence, in the modified Smith model, Curve 4, we let $G_0 = 0$ for all $\bar{\psi}$.

To explain the effect of G_0 on the neutral stability curves, we recall Eqs. (89) and (96), rewritten here for $r = 1$ and $\sigma = 0$,

$$\Lambda = 2U_0 G_N^2 + G_0 \quad (152)$$

$$\lambda_2 = -\frac{1}{2} [-\bar{V}_0 + \sqrt{\bar{V}_0^2 + 4\alpha^2}] \quad (153)$$

where $\bar{V}_0 = 0.8604$ for the Blasius flow. The disturbances decay like $\exp(-|\lambda_2|\bar{\psi})$ outside the boundary layer. From Eq. (153), we see that for small wavenumbers, $\alpha < 0.1$, $|\lambda_2| \ll 1$, and hence the disturbances decay very slowly as $\bar{\psi} \rightarrow \infty$. Therefore, changes in the basic-flow quantities outside the boundary layer affect the neutral stability characteristics for small wavenumbers. Furthermore, the term G_N^2 is proportional to the curvature of the inviscid streamlines. The presence of G_0 with G_N^2 in the same term, attaches the meaning of curvature to G_0 . Therefore, we can view Λ in Eq. (152) as a measure of the effective curvature that includes viscous effects. We note that for the Blasius flow and non-separating Falkner-Skan flows, G_0 is negative for all $\bar{\psi}$, as can be seen from Eq. (40e). It follows from Eq. (152) that G_N^2 takes a larger value when we include the negative quantity G_0 , Curve 2, than when we neglect it completely, as in the modified Smith model, Curve 4. For Curve 3, G_0 is slightly negative and it vanishes outside the boundary layer. However, for large wavenumbers or growing vortices (i.e., $\sigma > 0$) Eqs. (153) and (96) indicate that the disturbances decay very fast outside the boundary layer. Hence the effect of the term G_0 , which has more influence outside the boundary layer than inside it, should diminish.

This also follows from Eqs. (152) when the Görtler number G_N takes large values.

Finally, we note that $\bar{\psi}_m = 12$ was used for all the calculations presented in Fig. 4. The accuracy of the solution was tested against changes in $\bar{\psi}_m$. Increasing $\bar{\psi}_m$ up to 24 produced insignificant changes, $O(10^{-6})$, in both the eigenvalues and the eigenfunctions. Also, the effect of the accuracy of the basic-flow solution was evaluated by using a second-order finite-difference scheme with $\Delta\eta = 0.01$ instead of the fourth-order Runge-Kutta scheme with $\Delta\eta = 0.01$. For the test case $\alpha = 0.01$, the change in the eigenvalue was insignificant $O(10^{-5})$, while the changes in the maximum values of the eigenfunctions were about 7%. This is consistent with the fact that the eigenvalue is a global value while the eigenfunction is a point solution. As a further test on the eigenvalues obtained for all the cases presented in this chapter, the adjoint problem was solved and the obtained eigenvalues were compared with those of the basic system. The discrepancy between the two eigenvalues thus obtained was $O(10^{-5})$.

Table 1 gives the Görtler number, G_N , as a function of the wave-number, α , for the neutral stability, $\sigma = 0$, of the Blasius flow for the previously mentioned models.

B. Effect of Displacement Thickness

The perturbation procedure presented in Section V was used to account for the effect of changes in the basic flow due to the displaced body on the neutral stability of the Blasius flow. Equations (148)-(150) show that the corrections V_1 and G_1 depend explicitly on the Reynolds number Re . We let Re_x denote $Re\phi_0$. Figure 5 shows the neutral stability curves (the dashed lines) for the Blasius flow with correction

Table 1
Neutral Stability of the Blasius Flow,
Values of Görtler Number G_N as a Function of Wavenumber α

G_N α	Görtler Model	Present Model	Floryan- Saric Model	Modified Smith Model
1.00	3.0392	2.8238	2.7954	2.7629
0.90	2.6492	2.4366	2.4028	2.3662
0.80	2.2919	2.0829	2.0423	2.0008
0.70	1.9669	1.7623	1.7129	1.6619
0.60	1.6735	1.4747	1.4136	1.3606
0.50	1.4110	1.2200	1.1429	1.0834
0.40	1.1788	0.9981	0.8990	0.8332
0.30	0.9761	0.8100	0.6792	0.6088
0.25	0.8856	0.7290	0.5773	0.5060
0.20	0.8024	0.5672	0.4797	0.4090
0.15	0.7264	0.5947	0.3853	0.3176
0.10	0.6577	0.5418	0.2912	0.2305
0.09	0.6449	0.5323	0.2720	0.2133
0.08	0.6324	0.5233	0.2525	0.1961
0.07	0.6202	0.5146	0.2325	0.1788
0.06	0.6083	0.5063	0.2119	0.1613
0.05	0.5967	0.4983	0.1905	0.1435
0.04	0.5855	0.4907	0.1677	0.1249
0.03	0.5746	0.4835	0.1430	0.1053
0.025	0.5693	0.4800	0.1295	0.09482
0.020	0.5641	0.4766	0.1149	0.08365
0.015	0.5590	0.4732	0.09877	0.07144
0.010	0.5539	0.4700	0.08001	0.5752

due to displacement speed for $Re_x = 10^3$ and 10^4 . It is clear from Fig. 5 that, for a given Reynolds number and wavenumber, the displacement-thickness effect is destabilizing for the Blasius flow. This effect is pronounced for small wavenumbers, which is expected because the disturbances extend farther outside the boundary layer, and there the changes in the basic flow due to the displacement body are important. Figure 6 shows the ratio of the Görtler number with displacement thickness effect accounted for to the Görtler number when this effect is absent. For a given Reynolds number, this ratio can be viewed as the ratio of the square root of the corresponding critical curvatures.

C. Effect of Decaying Streamline Curvature

Herbert¹¹ presented results for the Görtler model with streamline curvatures decaying exponentially away from the wall. Therefore, the function $r(\bar{\psi})$ in Eq. (89) has the form

$$r = e^{-c\bar{\psi}} \quad (154)$$

where c is a constant. In this case, an analytic solution for the system (91) can be obtained. However, in a more general situation, the variation of the streamline curvature is not exponential and it may be known only numerically. Since the perturbation procedure of Section V is not restricted to analytic representations of the streamline curvature, we used it to obtain the correction to the Görtler number due the variation specified by Eq. (154) as an example. For this case, the integral (147a) was evaluated numerically while the integral (147b) was obtained analytically. Figure 7 shows the neutral stability curve for $c = 0.1$. The Görtler number in this figure is based on the curvature of the wall (i.e., at $\bar{\psi} = 0$). Also shown in Fig. 7 is the calculation of Herbert

using the Görtler model. We see that the decay of the streamline curvature stabilizes the flow. The stabilization effect is pronounced in the small wavenumber region. This is again because for small wavenumbers the disturbances extend farther outside the boundary layer. As noted by Herbert¹¹, the stabilizing effect of the decay in the streamline curvature from the value at the wall is due to the decrease in the driving centrifugal forces associated with the decreasing curvature.

D. Growth Rates for the Blasius Flow

Curves of constant growth rate were obtained for the Blasius flow. The results are plotted in Fig. 8, which gives the Görtler number G_N as a function of the wavenumber α . The difference between these curves and those obtained by Floryan and Saric appears only for $\sigma < 0.1$. This is because of the fast decay of the solution outside the boundary layer for $\sigma > 0.1$. Figures 9a-9c show the eigenfunctions u , v , and w , respectively, for the case of neutral stability (i.e., $\sigma = 0$) and for amplified vortices with $\sigma = 2.0$ at the wavenumber $\alpha = 0.5$. The Görtler numbers are 1.2200 for $\sigma = 0$ and 5.4523 for $\sigma = 2.0$. The persistence of the disturbance outside the boundary layer (i.e., $\bar{\psi} > 5$ where $U_0 \approx 0.99$) for the neutral stability case is clear from these figures. Also we note the large gradient of the solution near the wall for $\sigma = 2.0$. However, no orthonormalization was needed for the basic system while one orthonormalization at $\bar{\psi} = 2.328$ was needed for the adjoint system. As the growth rate increases, the number of orthonormalizations increases. The maximum number of orthonormalizations was 3 for the results of Fig. 8.

E. The Falkner-Skan Profiles

The Falkner-Skan profiles correspond to constant values of the pressure-gradient parameter β_0 defined in Eq. (34). For flows along walls with general curvature variation, the boundary-layer solution is nonsimilar. The consideration of the self-similar solutions in this section is an approximation. That is we patch the solution of the nonsimilar boundary layer to a self-similar profile that has the local value of the pressure-gradient parameter. This amounts to neglecting the history of the boundary layer up to the position under consideration and neglecting the gradient of β_0 at the local position.

Figure 10 shows the neutral stability curves for different values of the pressure-gradient parameter β_0 . Favorable pressure gradients (i.e., $\beta_0 > 0$) are stabilizing. For $\beta_0 = 0.1$, the Görtler number shows a minimum at $\alpha \approx 0.09$. Adverse pressure gradients have a destabilizing effect. This effect diminishes as the wavenumber increases. All wavenumbers smaller than a certain value that depends on β_0 appear to be unstable. For $\beta_0 = -0.05$, the wavenumber at which there is no solution (i.e., no Görtler number) for neutral stability is $\alpha \approx 0.024$ and for $\beta_0 = -0.1$ it is $\alpha \approx 0.048$. We attribute this behavior to the normal component of the basic flow which increases as the pressure gradient becomes more adverse. By considering neutral stability, we suppressed the change in the shape of the vortices in the downstream direction. This seems to be inconsistent with the growing boundary layer manifested by the transverse component V_0 . By considering a parallel stream in the basic state (i.e., using the Görtler model for which $V_0 = H_0 = G_0 = 0$ for all $\bar{\psi}$) and for $\beta_0 = -0.1$, we obtained a curve on the $G_N - \alpha$ chart that is very similar to the case of no pressure gradient and there is no

limiting wavenumber for neutral stability. The smallest wavenumber considered was 10^{-4} . The value of G_N approaches approximately 0.45 as $\alpha \rightarrow 0$.

Figure 11 shows the Görtler number for neutral stability as a function of β_0 in the range $-0.18 \leq \beta_0 \leq 0.1$ for $\alpha = 0.1$. The separation profile corresponds to $\beta_0 = -0.1988$. The stabilizing effect of favorable pressure gradients and the destabilizing effect of adverse pressure gradients are clear from this figure.

F. Flows over a Hump

We consider the curved wall given by Eq. (38). The inviscid flow solution was obtained by using Davis' method. The nonsimilar boundary-layer equations, Eqs. (31)-(33), were solved by using a second-order accurate finite-difference scheme with $\Delta\eta = 0.01$ and $\Delta\xi = 0.005$. The asymptotic condition (36) was applied at $\eta = 8.4$, which corresponds to $\bar{\psi} = 11.8$. This value of $\bar{\psi}$ was taken as $\bar{\psi}_m$ for the stability computations.

The numerical values of the wall considered are:

$$H^*/L^* = 0.01, \quad B = 10.0$$

The maximum concave curvature is

$$k^*L^* = 0.2716 \quad \text{at} \quad x^*/L^* = 0.845$$

The curvature is zero at $x^*/L^* = 0.915$. The maximum convex curvature is

$$k^*L^* = 1.0 \quad \text{at} \quad x^*/L^* = 1.0.$$

The pressure-gradient parameter β_0 for this wall is shown in Fig. 12, while the curvature variation is shown in Fig. 3.

Figure 13 shows the growth rate σ as a function of x^*/L^* for vortices having the wavelength $\lambda^*/L^* = 0.166$ and $Re = U_\infty^* \rho^* L^* / \mu^* = 5.74$

$\times 10^4$. These values correspond to neutral stability at $x^*/L^* = 0.4$. At this location $\beta_0 = -0.011$ and $k^*L^* = 0.00496$. We see from Fig. 13 that the vortices grow in strength in the downstream direction. The maximum growth rate appears at $x^*/L^* = 0.75$. At this location $\beta_0 = -0.01$ and $k^*L^* = 0.154$. Downstream of $x^*/L^* = 0.75$ the pressure gradient is favorable. The growth rate drops very rapidly to zero at $x^*/L^* \approx 0.83$. At this location $\beta_0 = 0.283$ and $k^*L^* = 0.2647$. Downstream of $x^*/L^* \approx 0.83$, the vortices decay due to the favorable pressure gradient. Also shown in Fig. 13 are the growth rates of the same vortices calculated by using the Blasius profile and self-similar (Falkner-Skan) profiles. The agreement among these curves is reasonable in the region where the pressure gradient is slightly adverse. However, in the region of favorable pressure gradient, the Blasius and Falkner-Skan profiles overpredict by great amount the growth rates. Thus, using nonsimilar profiles is a must in determining the stability over such surfaces.

Figure 14 shows the results corresponding to vortices having the wavelength $\lambda^*/L^* = 0.0247$ when $Re = 2.871 \times 10^5$. These values were chosen to obtain neutral stability at $x^*/L^* = 0.4$. The same general characteristics of the growth rate curve of the previous wavelength are also observed in this case.

REFERENCES

1. Görtler, H., "On the three-dimensional instability of laminar boundary layers on concave walls", NACA Tech. Memo. 1375, 1954, Translation of "Über eine dreidimensionale instabilität laminarer Grenzschichten an konkaven wänden", Ges. d. Wiss. Göttingen, Nachr. a.d. Math., Bd. 2, Nr. 1, 1940.
2. Wortman, F. X. "Visualization of transition", J. Fluid Mech. 38, 473-480, 1969.
3. Bippes, H., "Experimental study of the laminar-turbulent transition of a concave wall in a parallel flow", NASA TM-75243, 1978. Translation of "Experimentelle untersuchung laminar-turbulenten umschlags an einer parallel angeströmten konkaven wand", Heidelberger Akademie der Wissenschaften, Mathematisch-Naturwissenschaftliche Klasse, Sitzungsberichte, No. 3, 103-180, 1972.
4. Aihara, Y., "Transition in an incompressible boundary layer along a concave wall", Bul. Aero. Res. Inst. Tokyo Univ., 3, 143-160, 1961.
5. Tani, I. and Sakagami, J., "Boundary layer instability at subsonic speeds", Proc. Int. Counc. Aero. Sci., Stockholm, 1962. (Spartan, Washington, D.C., 1964).
6. Tani, I. and Aihara, Y., "Görtler vortices and boundary-layer transition," ZAMP, 20, 609-618, 1969.
7. Nayfeh, A. H., "Effect of streamwise vortices on Tollmien-Schlichting waves", VPI & SU, Department of Engineering Science and Mechanics, Rept. No. VPI-E-79.12, March 1979.
8. Hämmerlin, G., "Zur theorie der dreidimensionalen instabilität laminarer grenzschichten", ZAMP 7, 156-164, 1956.

9. Hämmerlin, G., "Über die stabilität einer kompressiblen strömung längs einer konkaven wand bei ver schiedenen wandtemperaturverhält- nissen", Deutsche Versuchsanstalt für Luftfahrt, Bericht 176, 1961.
10. Tobak, M., "On local Görtler instability", ZAMP, 22, 190-143, 1971.
11. Herbert, Th., "On the stability of the boundary layer along a concave wall", Arch. Mech. Stos, 28, 1039-1055, 1976.
12. Smith, A. M. O., "On the Growth of Taylor-Görtler vortices along highly concave walls", Quart. Appl. Math. 13, 233-262, 1955.
13. Floryan, M. M. and Saric, W. S., "Stability of Görtler vortices in boundary layers with suction", AIAA Paper No. 79-1497, presented at the 12th AIAA Fluid and Plasma Dynamics Conference, Williamsburg, Virginia, July 23-25, 1979.
14. Davis, R. T., "Numerical methods for coordinate generation based on Schwartz-Christoffel transformations", AIAA Paper NO. 79-1463, presented at the 4th Computational Fluid Dynamics Conference, Williamsburg, Virginia, July 23-24, 1979.
15. Schultz-Grunow, F. and Breuer, W., "Laminar boundary layers on cambered walls", In Basic Developments in Fluid Dynamics, 1, 377-436, Academic Press, New York and London, 1965.
16. Van Dyke, M. D., "Higher order boundary layer theory", Annual Rev. Fluid Mech. 1, 265-293, 1969.
17. Blottner, F. G., "Investigation of some finite-difference techniques for solving the boundary-layer equations", Computer Methods in Applied Mechanics and Engineering 6, 1-30, 1975.
18. Van Dyke, M. D., Perturbation methods in fluid mechanics, The Para- bolic Press, Stanford, California, 1964, Annotated edition 1975.

19. Kaplun, S., "The role of coordinate systems in boundary-layer theory", ZAMP, 5, 111-135, 1954.
20. Davis, R. T., "A study of the use of optimal coordinate in the solution of the Navier-Stokes equations", University of Cincinnati, Dept. of Aerospace Engineering, AFL 74-12-14, 1974.
21. Nayfeh, A. H., "Introduction to perturbation techniques", Wiley-Interscience, New York, (in press).
22. Scott, R. R. and Watts, H. A., "Computational solution of linear two-point boundary-value problems via orthonormalization", SIAM J. Num. Anal. 14, 40-70, 1977. Also, "SUPPORT--A computer code for two-point boundary-value problems via orthonormalization", SAND 75-0198.

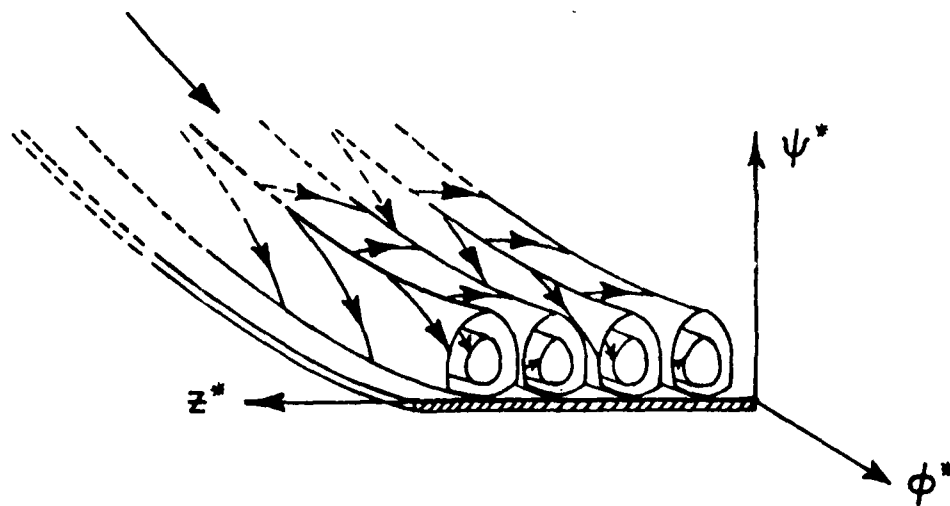


Figure 1. Görtler vortices in flow along a concave wall.

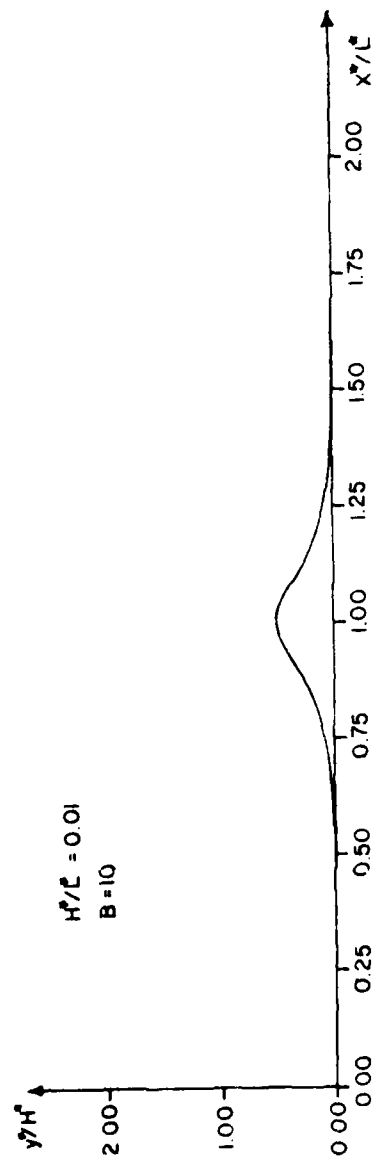


Figure 2. Geometry of the curved wall.

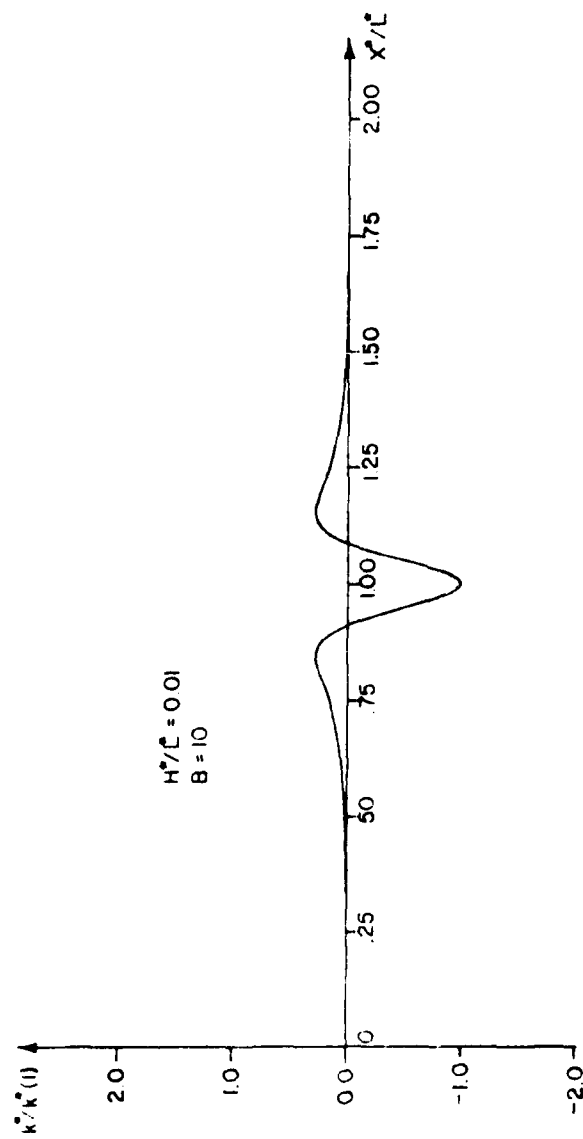


Figure 3. Wall curvature distribution.

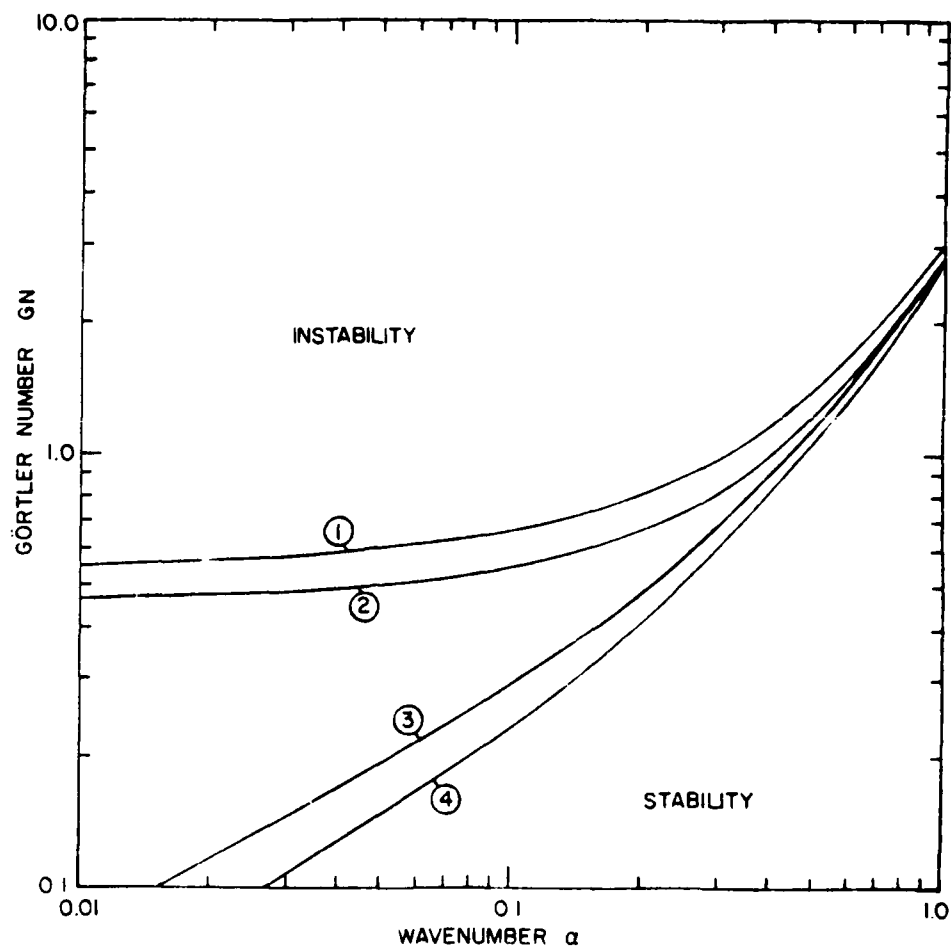


Figure 4. Neutral stability for the Blasius flow;
 (1) The Görtler model, (2) The present
 model, (3) Floryan-Saric model, (4) The
 modified Smith model.

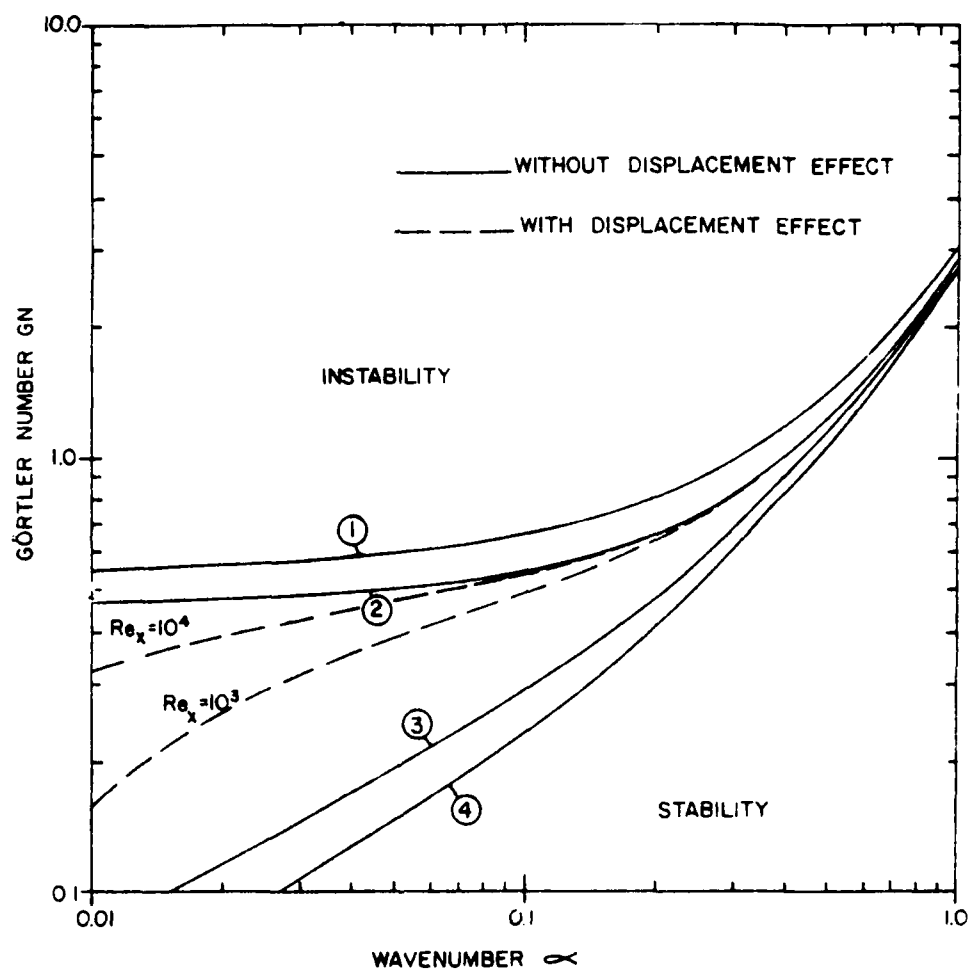


Figure 5. Neutral stability of the Blasius flow; effect of displacement thickness.

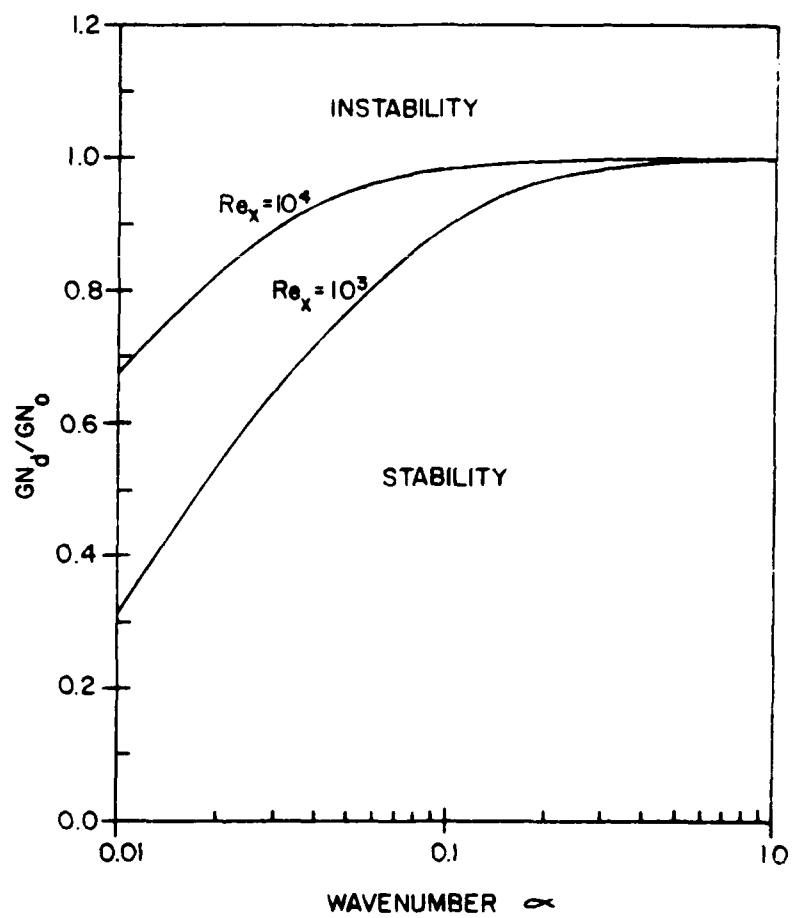


Figure 6. Neutral stability of the Blasius flow; ratio of the Görtler number with displacement effect to the Görtler number without displacement effect.

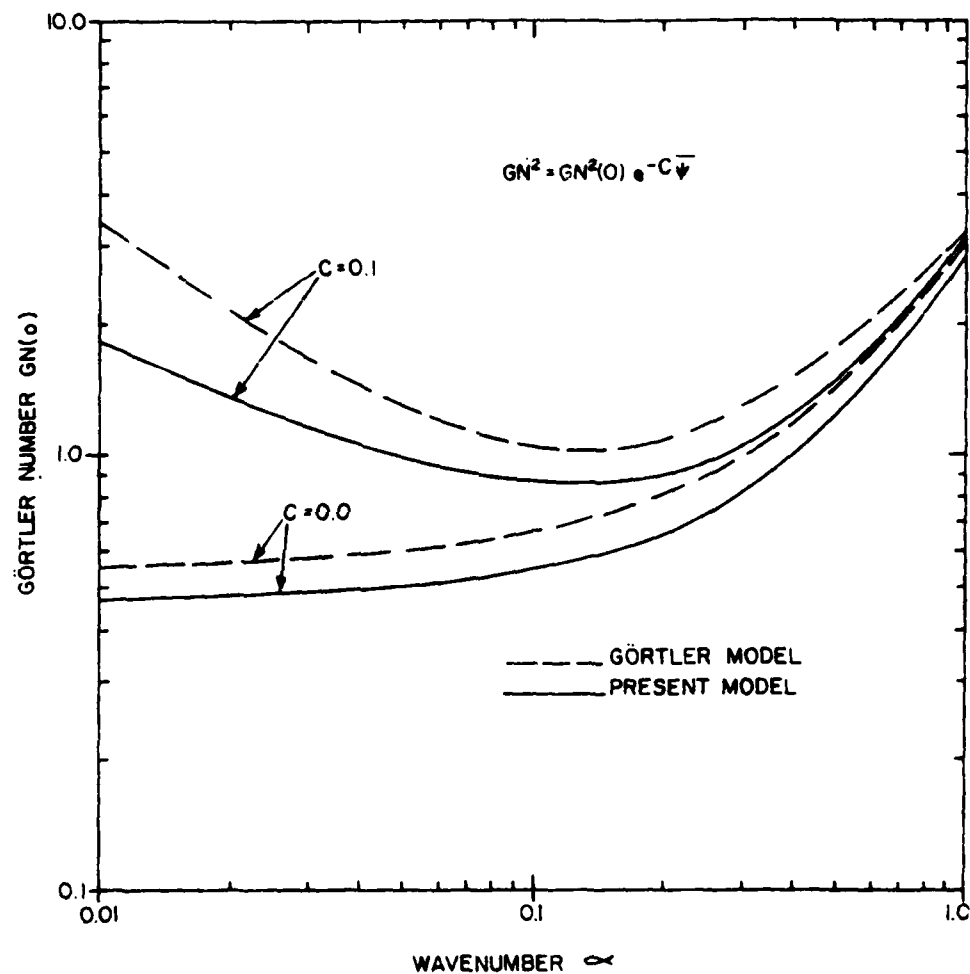


Figure 7. Neutral stability of the Blasius flow; effect of decaying streamline curvature.

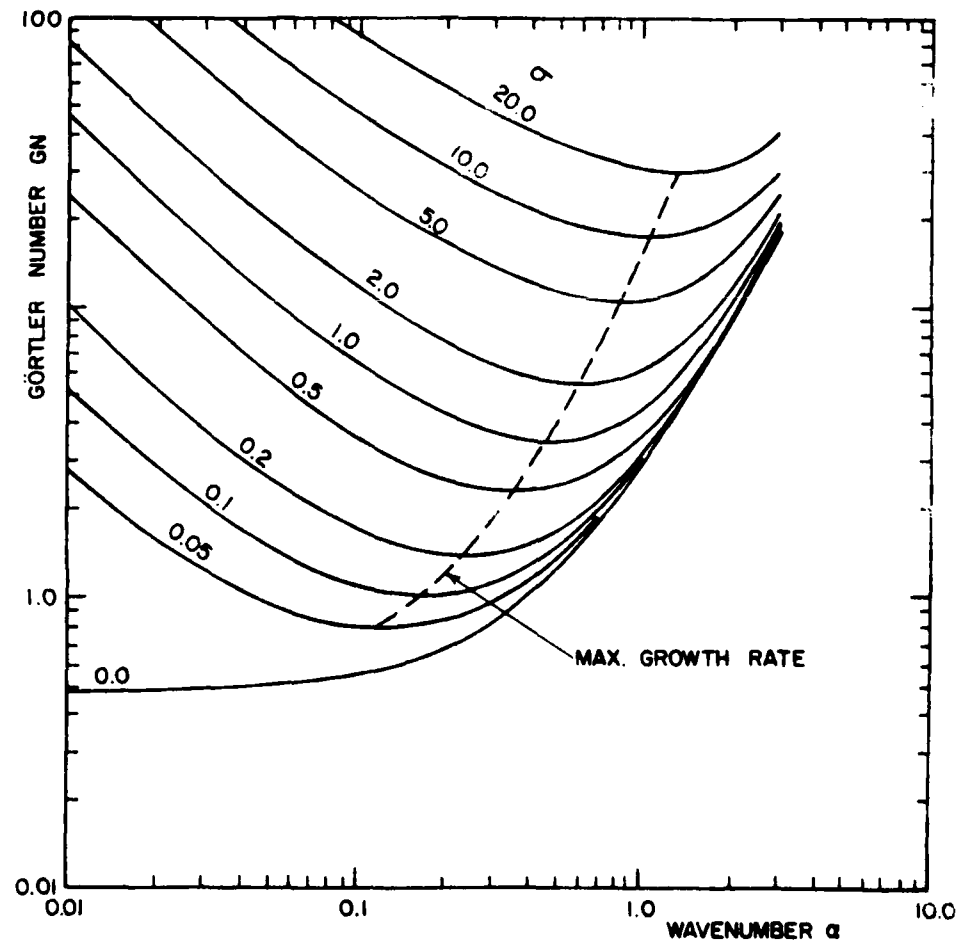


Figure 8. Curves of constant growth rate for the Blasius flow.

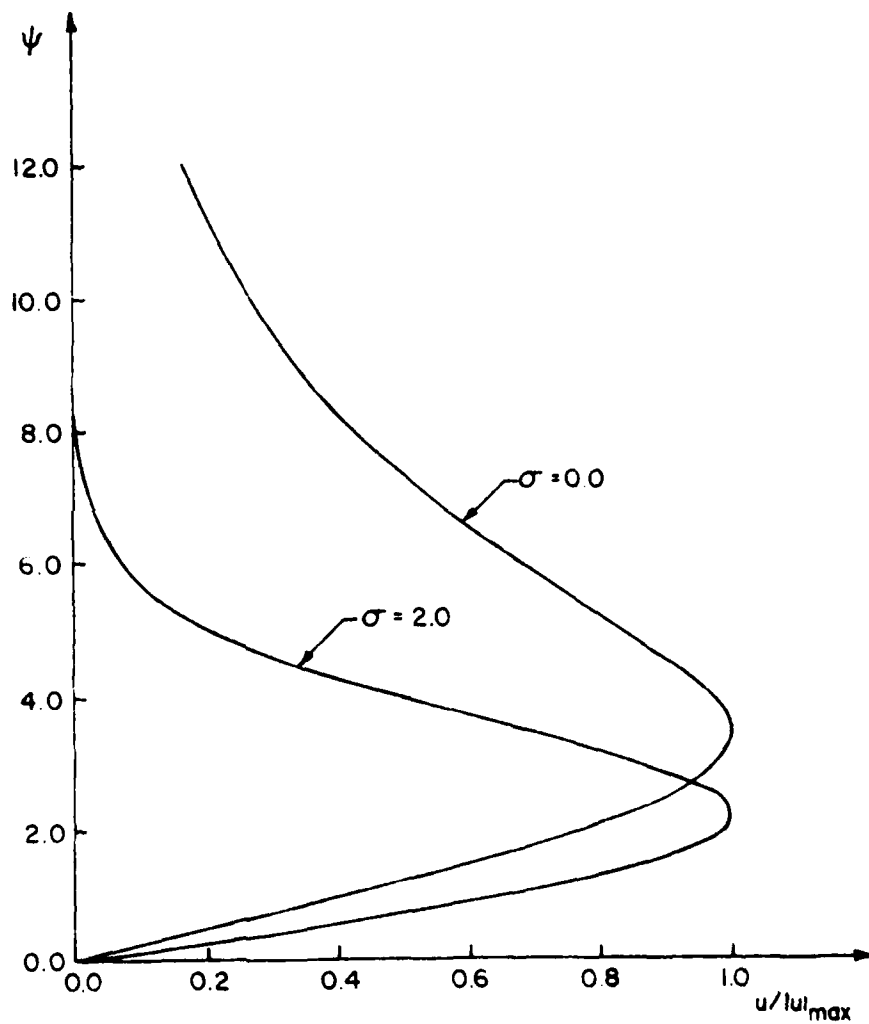


Figure 9a. Eigenfunctions for the Blasius flow;
the u -component.

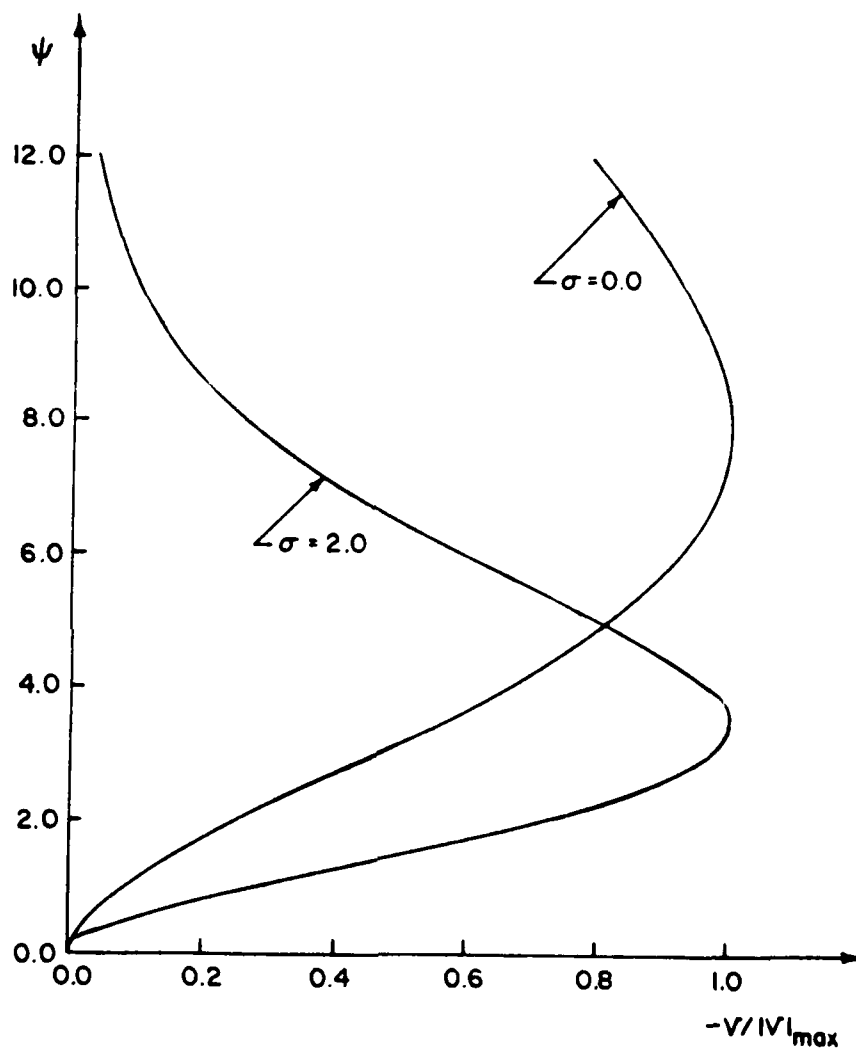


Figure 9b. Eigenfunctions for the Blasius flow;
the v-component.

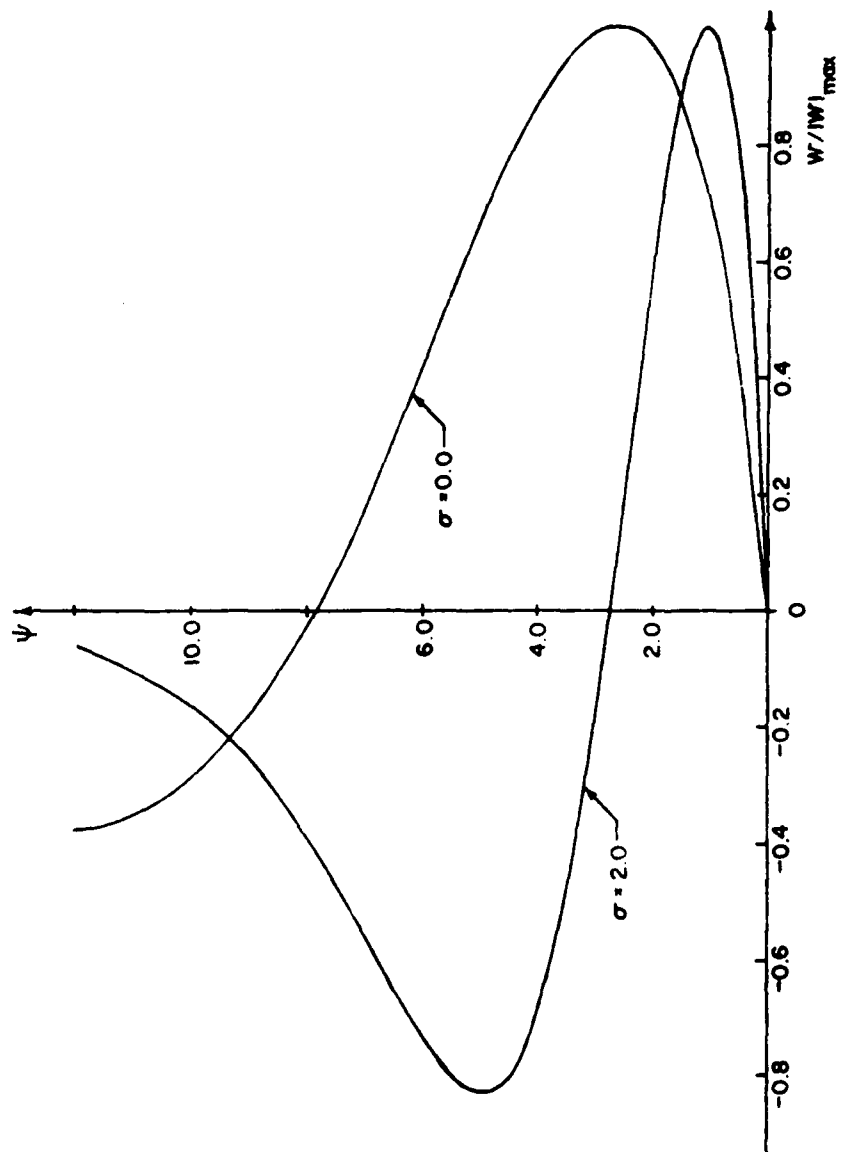


Figure 9c. Eigenfunctions for the Blasius flow;
the w-component.

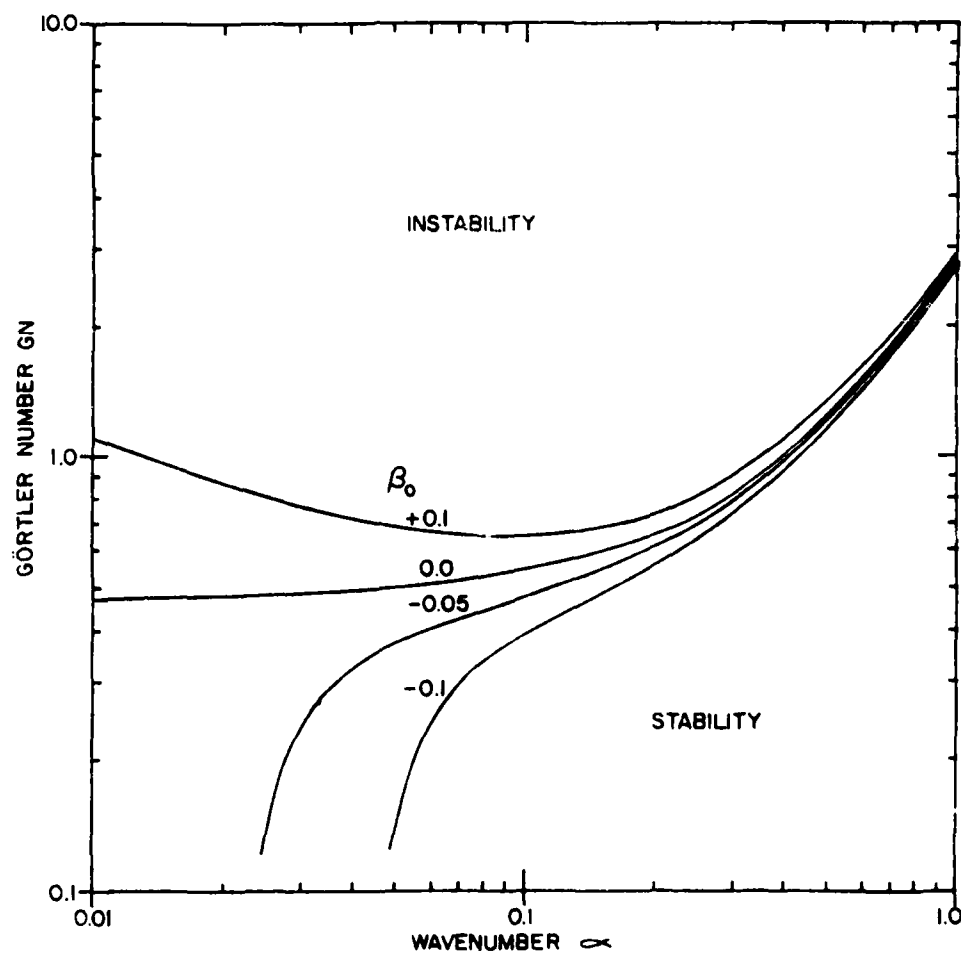


Figure 10. Neutral stability for the Falkner-Skan flows.

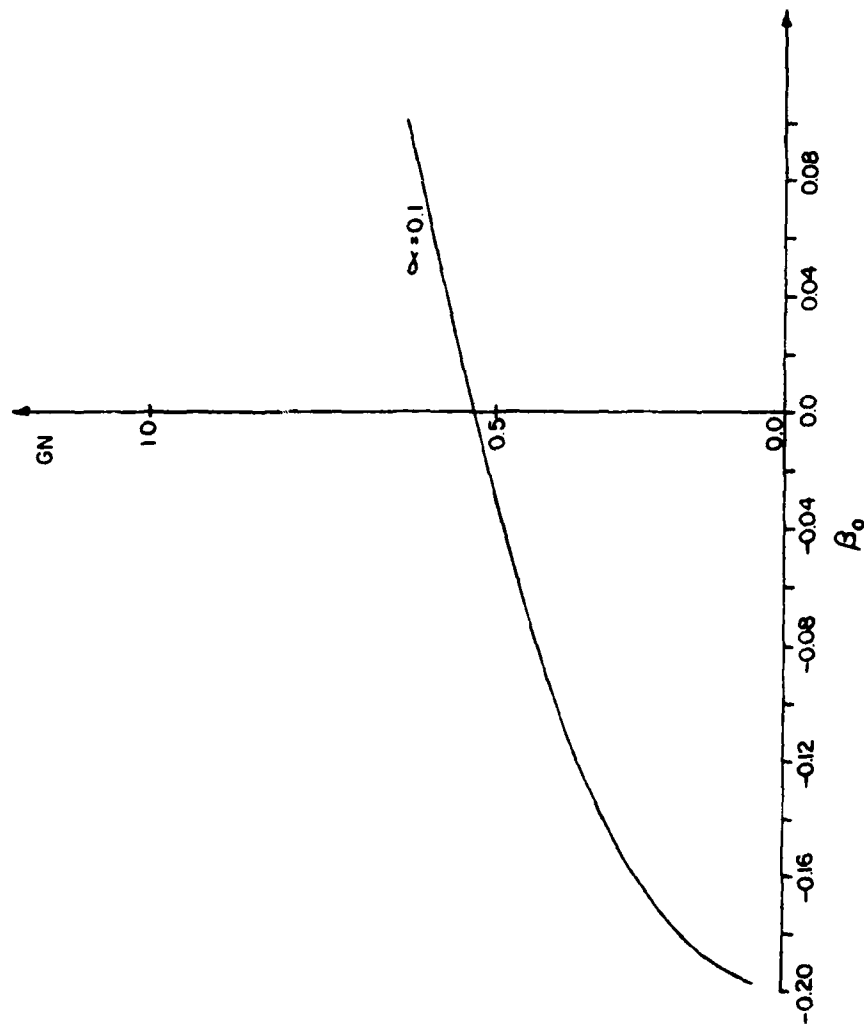


Figure 11. Neutral stability of the Falkner-Skan profiles for wavenumber $\alpha = 0.1$.

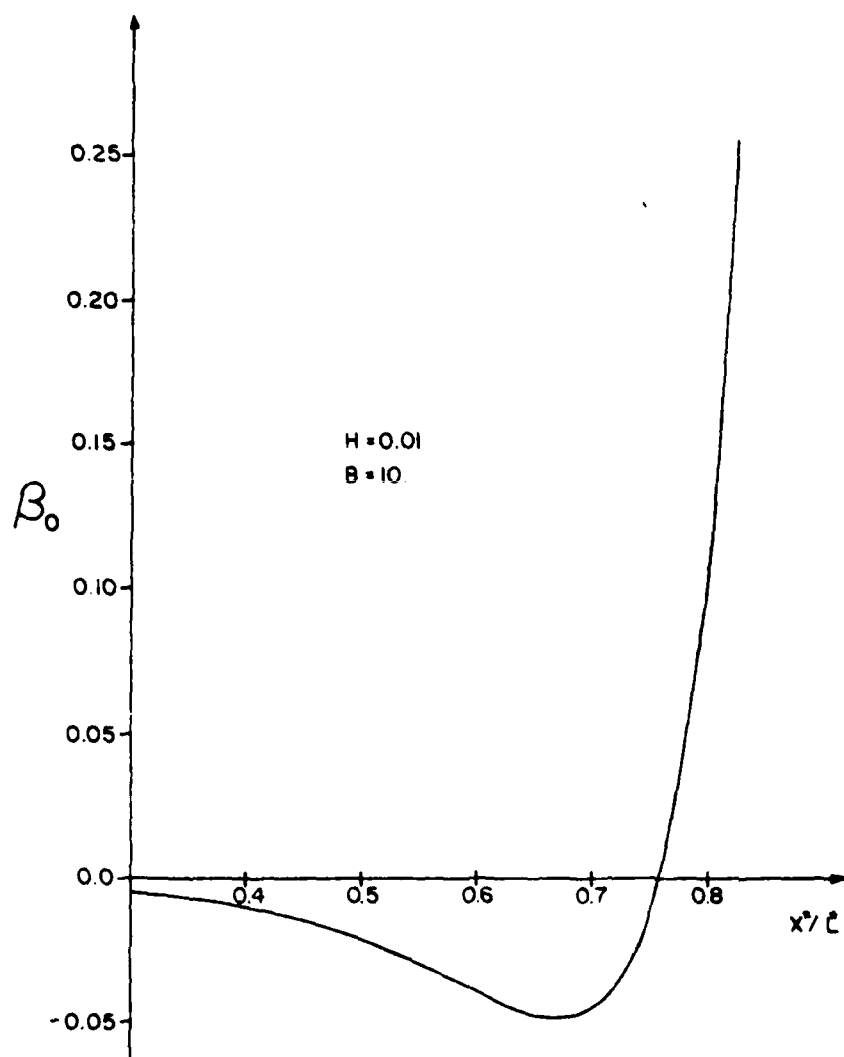


Figure 12. Distribution of the pressure-gradient parameter β_0 for the hump.

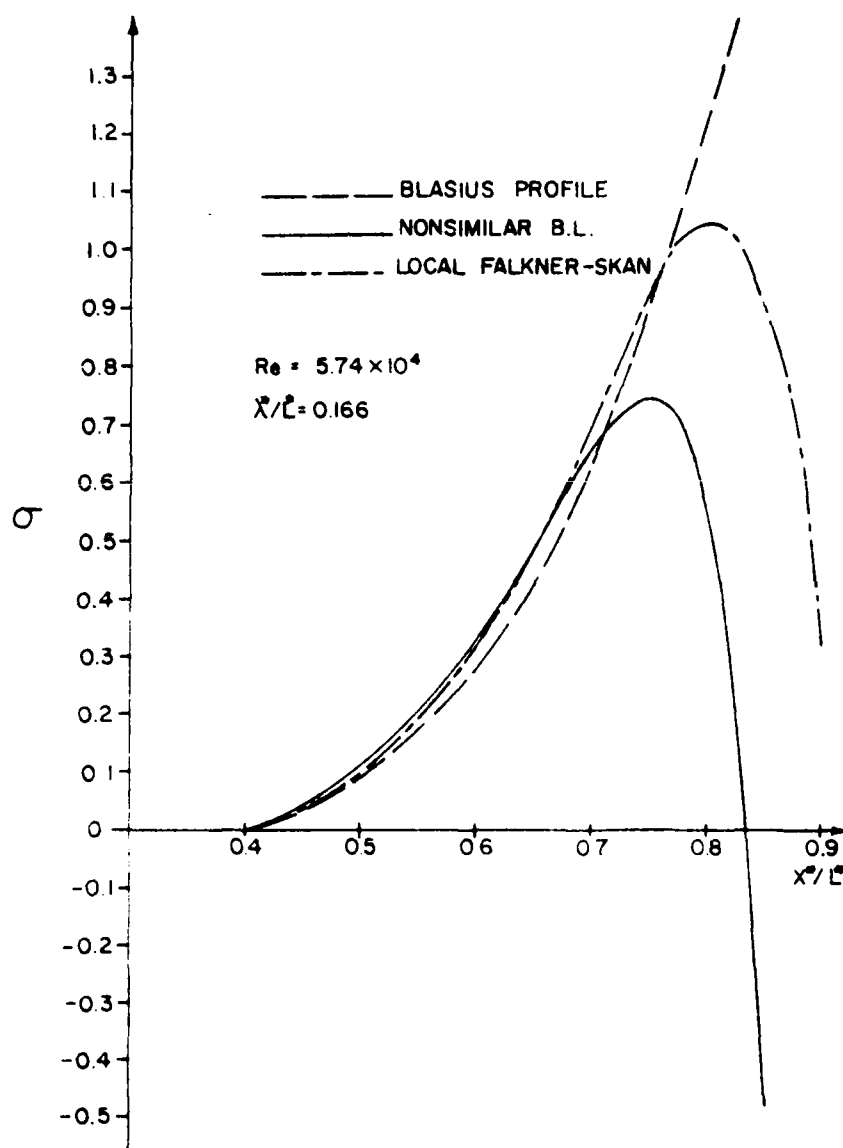


Figure 13. Growth rate of flows over a hump for wavelength $\lambda^*/L^* = 0.166$.

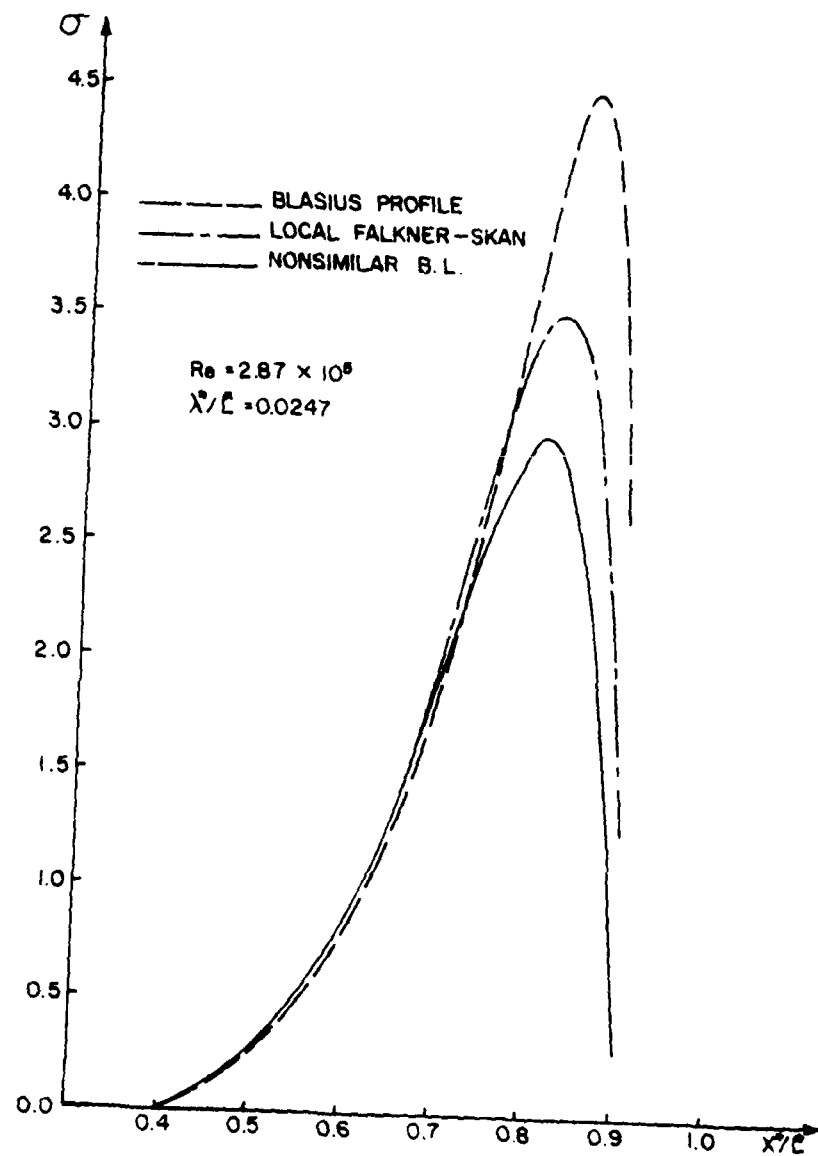


Figure 14. Growth rate of flows over a hump for wavelength $\lambda^*/L^* = 0.0247$.

APPENDIX A

The Navier-Stokes Equations in an Orthogonal Curvilinear Coordinate System

Let ϕ^* , ψ^* , and z^* denote an orthogonal curvilinear set of coordinates. This system is constructed from the cylindrical surfaces

$$\phi^*(x^*, y^*) = C_\phi \quad (A1)$$

$$\psi^*(x^*, y^*) = C_\psi \quad (A2)$$

and the planes

$$z^* = C_z \quad (A3)$$

where C_ϕ , C_ψ , C_z are constants. We consider a steady incompressible flow with constant properties. The equation of motion in the coordinate system (A1)-(A3) are¹⁹

ϕ^* -Momentum Equation

$$\begin{aligned} \frac{u}{h_\phi} \frac{\partial u}{\partial \phi} + \frac{v}{h_\psi} \frac{\partial u}{\partial \psi} + w \frac{\partial u}{\partial z} - v \left(\frac{v}{h_\phi h_\psi} \frac{\partial h_\psi}{\partial \phi} - \frac{u}{h_\phi h_\psi} \frac{\partial h_\phi}{\partial \psi} \right) = & - \frac{1}{h_\phi} \frac{1}{\rho} \frac{\partial p}{\partial \phi} \\ & + \frac{v}{h_\phi h_\psi} \frac{\partial}{\partial \phi} \left(2 \frac{h_\psi}{h_\phi} \frac{\partial u}{\partial \phi} + 2 \frac{v}{h_\phi} \frac{\partial h_\phi}{\partial \psi} \right) + \frac{\partial}{\partial \psi} \left[h_\psi \frac{\partial}{\partial \phi} \left(\frac{v}{h_\phi} \right) + \frac{h^2}{h_\psi} \frac{\partial}{\partial \psi} \left(\frac{u}{h_\phi} \right) \right] \\ & + h_\phi h_\psi \frac{\partial^2 u}{\partial z^2} + h_\psi \frac{\partial^2 w}{\partial \phi \partial z} + \left[\frac{h_\psi}{h_\phi} \frac{\partial}{\partial \phi} \left(\frac{v}{h_\psi} \right) + \frac{h_\phi}{h_\psi} \frac{\partial}{\partial \psi} \left(\frac{u}{h_\phi} \right) \right] \cdot \frac{\partial h_\phi}{\partial \psi} \\ & - 2 \left(\frac{1}{h_\psi} \frac{\partial v}{\partial \psi} + \frac{u}{h_\phi h_\psi} \frac{\partial h_\psi}{\partial \phi} \right) \cdot \frac{\partial h_\psi}{\partial \phi} \end{aligned} \quad (A4)$$

ψ^* -Momentum Equation

$$\begin{aligned}
 \frac{u}{h_\phi} \frac{\partial v}{\partial \phi} + \frac{v}{h_\psi} \frac{\partial v}{\partial \psi} + w \frac{\partial v}{\partial z} + u \left(\frac{v}{h_\phi h_\psi} \frac{\partial h_\psi}{\partial \phi} - \frac{u}{h_\phi h_\psi} \frac{\partial h_\phi}{\partial \psi} \right) = & - \frac{1}{h_\psi} \frac{1}{\rho} \frac{\partial p}{\partial \psi} \\
 + \frac{v}{h_\phi h_\psi} \frac{\partial}{\partial \phi} \left[\frac{h_\psi^2}{h_\phi} \frac{\partial}{\partial \phi} \left(\frac{v}{h_\psi} \right) + h_\phi \frac{\partial}{\partial \psi} \left(\frac{u}{h_\phi} \right) \right] + \frac{\partial}{\partial \psi} \left(2 \frac{h_\phi}{h_\psi} \frac{\partial v}{\partial \psi} + 2 \frac{u}{h_\psi} \frac{\partial h_\psi}{\partial \phi} \right) \\
 + h_\phi \frac{\partial^2 w}{\partial \psi \partial z} + h_\phi h_\psi \frac{\partial^2 v}{\partial z^2} + \left[\frac{h_\psi}{h_\phi} \frac{\partial}{\partial \phi} \left(\frac{v}{h_\psi} \right) + \frac{h_\phi}{h_\psi} \frac{\partial}{\partial \psi} \left(\frac{u}{h_\phi} \right) \right] \cdot \frac{\partial h_\psi}{\partial \phi} \\
 - 2 \left(\frac{1}{h_\phi} \frac{\partial u}{\partial \phi} + \frac{v}{h_\phi h_\psi} \frac{\partial h_\phi}{\partial \psi} \right) \frac{\partial h_\phi}{\partial \psi}
 \end{aligned} \tag{A5}$$

z^* -Momentum Equation

$$\begin{aligned}
 \frac{u}{h_\phi} \frac{\partial w}{\partial \phi} + \frac{v}{h_\psi} \frac{\partial w}{\partial \psi} + w \frac{\partial w}{\partial z} = & - \frac{1}{\rho} \frac{\partial p}{\partial z} + \frac{v}{h_\phi h_\psi} \frac{\partial}{\partial \phi} \left(h_\psi \frac{\partial u}{\partial z} + \frac{h_\psi}{h_\phi} \frac{\partial w}{\partial \phi} \right) \\
 + \frac{\partial}{\partial \psi} \left(\frac{h_\phi}{h_\psi} \frac{\partial w}{\partial \psi} + h_\phi \frac{\partial v}{\partial z} \right) + 2 h_\phi h_\psi \frac{\partial^2 w}{\partial z^2}
 \end{aligned} \tag{A6}$$

Continuity Equation

$$\frac{\partial}{\partial \phi} (h_\psi u) + \frac{\partial}{\partial \psi} (h_\phi v) + h_\phi h_\psi \frac{\partial w}{\partial z} = 0 \tag{A7}$$

All the variables in the above equations are dimensional; we dropped the asterisks for simpler notation. Where u^* , v^* and w^* are the velocity components in the ϕ^* , ψ^* , and z^* directions respectively; p^* , ρ^* and ν^* are the static pressure, density, and kinematic viscosity respectively; h_ϕ^* and h_ψ^* are the metric coefficients for the curves given by Eq. (A1) and (A2).

The Navier-Stokes equations when ϕ^* and ψ^* are the potential and stream functions of a two-dimensional incompressible irrotational flow become

ϕ^* -Momentum Equation

$$\begin{aligned} hu \frac{\partial u}{\partial \phi} + hv \frac{\partial u}{\partial \psi} + h^2 w \frac{\partial u}{\partial z} - v^2 \frac{\partial h}{\partial \phi} + uv \frac{\partial h}{\partial \psi} = - \frac{h}{\rho} \frac{\partial p}{\partial \phi} + v[\nabla^2 u - \frac{u}{h} (\frac{\partial^2 h}{\partial \phi^2} \\ + \frac{\partial^2 h}{\partial \psi^2}) + \frac{2}{h} (\frac{\partial h}{\partial \psi} \frac{\partial v}{\partial \phi} - \frac{\partial h}{\partial \phi} \frac{\partial v}{\partial \psi})] \end{aligned} \quad (A8)$$

ψ^* -Momentum Equation

$$\begin{aligned} hu \frac{\partial v}{\partial \phi} + hv \frac{\partial v}{\partial \psi} + h^2 w \frac{\partial v}{\partial z} - u^2 \frac{\partial h}{\partial \psi} + uv \frac{\partial h}{\partial \phi} = - \frac{h}{\rho} \frac{\partial p}{\partial \psi} + v[\nabla^2 v - \frac{v}{h} (\frac{\partial^2 h}{\partial \phi^2} \\ + \frac{\partial^2 h}{\partial \psi^2}) + \frac{2}{h} (\frac{\partial h}{\partial \phi} \frac{\partial u}{\partial \psi} - \frac{\partial h}{\partial \psi} \frac{\partial u}{\partial \phi})] \end{aligned} \quad (A9)$$

z^* -Momentum Equation

$$hu \frac{\partial w}{\partial \phi} + hv \frac{\partial w}{\partial \psi} + h^2 w \frac{\partial w}{\partial z} = - \frac{h^2}{\rho} \frac{\partial p}{\partial z} + v \nabla^2 w \quad (A10)$$

Continuity Equation

$$\frac{\partial hu}{\partial \phi} + \frac{\partial hv}{\partial \psi} + h^2 \frac{\partial w}{\partial z} = 0 \quad (A11)$$

where

$$h = h_{\phi} = h_{\psi}$$

$$\nabla^2 = \frac{\partial^2}{\partial \phi^2} + \frac{\partial^2}{\partial \psi^2} + h^2 \frac{\partial^2}{\partial z^2}$$

Appendix B

Schwarz-Christoffel Transformations for Curved Surfaces

Davis¹⁴ presented a numerical method for integrating Schwarz-Christoffel transformations for curved surfaces. Sufficient information about the method and several examples are given by Davis.

Here, we specialize his method for the wall given by Eq. (38), that is

$$y = H \operatorname{sech} B(1 - x) \quad \text{for} \quad |x| < \infty \quad (B1)$$

We assume that the wall is specified by Eq. (B1) in the interval $0 \leq x \leq 2$ and it coincides with the x-axis outside that interval. For the case treated in Section II, $H = 0.01$ and $B = 10$, hence

$$y(0)/H = y(2)/H = 2e^{-10} \ll 1$$

Therefore the above assumption is justified.

We divide the wall in the interval $0 \leq x \leq 2$ into a finite number of elements N . Let

$$z_m = x_m + iy_m \quad (B2)$$

denote the left-end point of the m th element,

$$\beta_m = -\tan^{-1}\left(\frac{dy}{dx}\right)_m \quad (B3)$$

denote the angle between the tangent line and the x-axis (positive clockwise) at z_m , and

$$\theta_m = -\tan^{-1}\left(\frac{y_{m+1} - y_m}{x_{m+1} - x_m}\right) \quad (B4)$$

denote the angle between the straight line connecting the m th and $(m+1)$ th points on the wall and the x-axis (positive clockwise). As shown by Davis¹⁴, a transformation which maps the upper half of the

ζ -plane onto the region above the curved wall in the z -plane is

$$\frac{dz}{d\zeta} = M \prod_{m=1}^N \frac{C_{2m}/\pi}{g_{2m}} \frac{C_{3m}/\pi}{g_{3m}} \quad (B5)$$

where

$$C_{3m} = 4 \left(\frac{\beta_m + \beta_{m+1}}{2} - \theta_m \right) / (b_{m+1} - b_m)^2 \quad (B6)$$

$$C_{2m} = \frac{\beta_{m+1} - \beta_m}{b_{m+1} - b_m} - (b_{m+1} + b_m) C_{3m} \quad (B6)$$

$$g_{2m} = A_m / A_{m+1} \quad (B7)$$

$$g_{3m} = B_m / B_{m+1} \quad (B8)$$

$$A_m = (\zeta - b_m)^{(\zeta - b_m) b_m} e^{b_m} \quad (B9)$$

$$B_m = (\zeta - b_m)^{(\zeta^2 - b_m^2) (\zeta + b_m)^2 / 2} e^{b_m} \quad (B10)$$

Here the b_m are images of the z_m in the ζ -plane; they are real numbers.

The unknowns in Eq. (B5) are M and the b_m . They are determined iteratively as follows:

- (a) We guess values for the b_m and M . In the present application M is purely real; however, this need not be specified since it will come from the solution procedure automatically.

The b_m are picked such that $b_{m-1} < b_m < b_{m+1}$.

- (b) By using complex arithmetic, we integrate Eq. (B5). We set $b_1 = 0$ (i.e., the point $z = 0$ is transformed to $\zeta = 0$). Now the obtained z_{gm} will not coincide with the actual z_m given by Eq. (B2). A correction to M is obtained first by requiring that the point $z = (1.0, H)$ be transformed to the point

$\zeta = (1.0, 0)$. Updated values for the b_m are obtained from

$$\frac{b_{cm} - b_{cm-1}}{b_{gm} - b_{gm-1}} = k \frac{|z_m - z_{m-1}|}{|z_{gm} - z_{gm-1}|} \quad (B11)$$

where the subscript c denotes corrected or updated values and the subscript g denotes guessed or old values. The scale k is related to M by

$$k = \left| \frac{M_g}{M_c} \right|$$

- c. A new iteration is performed by using the new values of M and the b_m (step a). Step (b) is repeated until convergence is achieved.

The complex velocity in the z-plane is obtained as follows. Let

$$\frac{dz}{d\zeta} = Mf(\zeta; b_m) \quad (B12)$$

In the ζ -plane the flow is a uniform stream parallel to the ξ -axis.

Hence

$$\frac{dw}{d\zeta} = V \quad (B13)$$

where w is the complex potential. In the z-plane

$$(u - iv)_z = \frac{dw}{dz} = \frac{dw}{d\zeta} \frac{1}{dz/d\zeta}$$

$$(u - iv)_z = \frac{V}{Mf} \quad (B14)$$

Since $\sum_{m=1}^N \beta_m = 0$ then $f \rightarrow 1$ as $\zeta \rightarrow \infty$. The uniform flow in the ζ -plane is mapped onto a uniform flow in the z-plane. Hence

$$U = \frac{V}{M} \quad (B15)$$

Substituting Eq. (B15) into Eq. (B14) we obtain

$$u - iv = \frac{U}{f} \quad (B16)$$

In the actual calculations $U = 1$. The metric coefficient h is thus given by

$$h = |f| \quad (B17)$$

Appendix C

The Matrix ΔA

The matrix ΔA is a 6×6 square matrix. The non-zero elements of this matrix are

$$a_{21} = (h^2 - 1)\alpha^2 - V_0 h K_\psi - \frac{\delta_0}{R} \frac{d\sigma}{d\phi} - \frac{1}{R^2} (\sigma^2 + \frac{1}{2} \beta_0^2 - \beta_0 \sigma - \phi_0 \frac{\nabla^2 h}{h}) \quad (C1)$$

$$a_{23} = \frac{1}{R^2} (\beta_0 V_0 + 2\sigma h K_\psi - \beta_0 h K_\psi) \quad (C2)$$

$$a_{24} = \frac{\beta_0 h \alpha}{R^2} \quad (C3)$$

$$a_{26} = \frac{\sigma}{R^2} \quad (C4)$$

$$a_{33} = h K_\psi \quad (C5)$$

$$a_{34} = - (h - 1)\alpha \quad (C6)$$

$$a_{54} = (h^2 - 1)\alpha^2 - \frac{\delta_0}{R} \frac{d\sigma}{d\phi} - \frac{\sigma^2}{R^2} \quad (C7)$$

$$a_{56} = - (h - 1)\alpha \quad (C8)$$

$$a_{61} = \frac{1}{2} \beta_0 h K_\psi + \sigma h K_\psi + \frac{1}{2} \beta_0' - 2U_0 (h - 1) G_N^2 \quad (C9)$$

$$a_{63} = -(h^2 - 1)\alpha^2 - 2V_0 h K_\psi + (h K_\psi)' + h^2 K_\psi^2 + \frac{\delta_0}{R} \frac{d\sigma}{d\phi} + \frac{\sigma^2}{R^2} - \frac{\phi_0}{R^2} \frac{\nabla^2 h}{h} \quad (C10)$$

$$a_{64} = V_0 (h - 1)\alpha \quad (C11)$$

$$a_{65} = - (h - 1)\alpha \quad (C12)$$

$$a_{66} = -h K_\psi \quad (C13)$$

The prime denotes differentiation with respect to $\bar{\psi}$.

Appendix D
The Matrices P and P^*

These matrices are given in the next two pages.

P =

$$\begin{bmatrix} 0 & 0 & x_1 & 0 & 0 & x_2 \\ 0 & 0 & \lambda_2 x_1 & 0 & 0 & \lambda_5 x_2 \\ 1 & 1 & 0 & 1 & 1 & 0 \\ -1 & -\lambda_2/\alpha & -(\gamma + \sigma x_1)/\alpha & 1 & -\lambda_5/\alpha & -(\gamma + \sigma x_2)/\alpha \\ -\alpha & -\lambda_2^2/\alpha & -\lambda_2(2\gamma + \sigma x_1)/\alpha & -\alpha & -\lambda_5^2/\alpha & -\lambda_5(2\gamma + \sigma x_2)/\alpha \\ -(\bar{V}_0 + \sigma/\alpha) & 0 & \gamma(2\alpha^2 + 2\sigma + \lambda_2 \bar{V}_0)/\alpha^2 & -(\bar{V}_0 - \sigma/\alpha) & 0 & \gamma(2\alpha^2 + 2\sigma + \lambda_5 \bar{V}_0)/\alpha^2 \end{bmatrix}$$

where $\gamma = 2G_N^2 + \bar{G}_0$

$$x_1 = -(\bar{V}_0/\alpha^2)[2\alpha^2 + 2\sigma + \lambda_2 \bar{V}_0 - \sigma(1 - 2\lambda_2/\bar{V}_0)]$$

$$x_2 = -(\bar{V}_0/\alpha^2)[2\alpha^2 + 2\sigma + \lambda_5 \bar{V}_0 - \sigma(1 - 2\lambda_5/\bar{V}_0)]$$

λ_2 and λ_5 are defined by Eqs. (96a) and (96b)

$$\sigma \neq \alpha \bar{V}_0$$

$$P^* =$$

$$\begin{bmatrix} \sigma x_2 - (\bar{V}_0 + \alpha)x_1 & 1 & y_1 & \sigma x_4 - (\bar{V}_0 - \alpha)x_3 & 1 & y_2 \\ x_1 & -\lambda_1^*/(\alpha^2 + \sigma) & 0 & x_3 & -\lambda_1^*/(\alpha^2 + \sigma) & 0 \\ (\alpha + \sigma/\alpha)x_2 & 0 & (\alpha^2 + \sigma)/\lambda_1^* & -(\alpha + \sigma/\alpha)x_4 & 0 & (\alpha^2 + \sigma)/\lambda_1^* \\ -\bar{V}_0 x_2 & 0 & -\sigma/\alpha & \bar{V}_0 x_4 & 0 & -\sigma/\alpha \\ x_2 & 0 & \lambda_1^*/\alpha & -x_4 & 0 & \lambda_1^*/\alpha \\ x_2 & 0 & 1 & x_4 & 0 & 1 \end{bmatrix}$$

where $x_1 = \gamma^* + \sigma^2/\alpha$, $x_2 = \sigma - \alpha\bar{V}_0$, $x_3 = \gamma^* - \sigma^2/\alpha$, $x_4 = \sigma + \alpha\bar{V}_0$

$$y_n = \sigma + \lambda_n^*[\gamma^* + \sigma(\alpha^2 + \sigma)/\lambda_n^* - \sigma\lambda_n^*]/(\alpha^2 + \sigma + \lambda_n^{*2}), \quad n = 1, 2$$

and

$$\gamma^* = 2G_N^2 + \bar{G}_0 - \sigma\bar{V}_0, \quad \lambda_1^* = -\lambda_5, \quad \lambda_2^* = -\lambda_2$$

λ_2 and λ_5 are defined by Eqs. (96a) and (96b)

$$\sigma \neq \alpha\bar{V}_0$$

BIBLIOGRAPHIC DATA SHEET	1. Report No.	2.	3. Recipient's Accession No.
4. Title and Subtitle On Görtler Instability		5. Report Date December 1979	
7. Author(s)		6.	
9. Performing Organization Name and Address Virginia Polytechnic Institute and State University Blacksburg, VA 24061		8. Performing Organization Rept. No. VPI-E-79.41	
		10. Project/Task/Work Unit No.	
		11. Contract/Grant No. N00014-75-C-0381	
12. Sponsoring Organization Name and Address Office of Naval Research 800 North Quincy Street Arlington, VA 22217		13. Type of Report & Period Covered Research Report	
		14.	
15. Supplementary Notes			
16. Abstracts Görtler instability for boundary-layer flows over generally curved walls is considered. The full linearized disturbance equations are obtained in an orthogonal curvilinear coordinate system. A perturbation procedure to account for second-order effects is used to determine the effects of the displacement thickness and the variation of the streamline curvature on the neutral stability of the Blasius flow. The pressure gradient in the mean flow is accounted for by solving the non-similar boundary-layer equations. Growth rates are obtained for the actual mean flow and compared with those for the Blasius flow and the Falkner-Skan flows. The results demonstrate the strong influence of the pressure gradient and the nonsimilarity of the basic flow on the stability characteristics.			
17. Key Words and Document Analysis. 17a. Descriptors Stability Görtler Transition			
17b. Identifiers/Open-Ended Terms			
17c. COSATI Field Group			
18. Availability Statement		19. Security Class (This Report) UNCLASSIFIED	21. No. of Pages
		20. Security Class (This Page) UNCLASSIFIED	22. Price

INSTRUCTIONS FOR COMPLETING FORM NTIS-35

(Bibliographic Data Sheet based on COSATI

Guidelines to Format Standards for Scientific and Technical Reports Prepared by or for the Federal Government, PB-180 600).

1. **Report Number.** Each individually bound report shall carry a unique alphanumeric designation selected by the performing organization or provided by the sponsoring organization. Use uppercase letters and Arabic numerals only. Examples FASEB-NS-73-87 and FAA-RD-73-09.
2. Leave blank.
3. **Recipient's Accession Number.** Reserved for use by each report recipient.
4. **Title and Subtitle.** Title should indicate clearly and briefly the *subject coverage* of the report, subordinate subtitle to the main title. When a report is prepared in more than one volume, repeat the primary title, add volume number and include subtitle for the specific volume.
5. **Report Date.** Each report shall carry a date indicating at least month and year. Indicate the basis on which it was selected (e.g., date of issue, date of approval, date of preparation, date published).
6. **Performing Organization Code.** Leave blank.
7. **Author(s).** Give name(s) in conventional order (e.g., John R. Doe, or J. Robert Doe). List author's affiliation if it differs from the performing organization.
8. **Performing Organization Report Number.** Insert if performing organization wishes to assign this number.
9. **Performing Organization Name and Mailing Address.** Give name, street, city, state, and zip code. List no more than two levels of an organizational hierarchy. Display the name of the organization exactly as it should appear in Government indexes such as Government Reports Index (GRI).
10. **Project/Task/Work Unit Number.** Use the project, task and work unit numbers under which the report was prepared.
11. **Contract/Grant Number.** Insert contract or grant number under which report was prepared.
12. **Sponsoring Agency Name and Mailing Address.** Include zip code. Cite main sponsors.
13. **Type of Report and Period Covered.** State interim, final, etc., and, if applicable, inclusive dates.
14. **Sponsoring Agency Code.** Leave blank.
15. **Supplementary Notes.** Enter information not included elsewhere but useful, such as: Prepared in cooperation with . . . Translation of . . . Presented at conference of . . . To be published in . . . Supersedes . . . Supplements . . . Cite availability of related parts, volumes, phases, etc. with report number.
16. **Abstract.** Include a brief (200 words or less) factual summary of the most significant information contained in the report. If the report contains a significant bibliography or literature survey, mention it here.
17. **Key Words and Document Analysis.** (a). **Descriptors.** Select from the Thesaurus of Engineering and Scientific Terms the proper authorized terms that identify the major concept of the research and are sufficiently specific and precise to be used as index entries for cataloging.
(b). **Identifiers and Open-Ended Terms.** Use identifiers for project names, code names, equipment designators, etc. Use open-ended terms written in descriptor form for those subjects for which no descriptor exists.
(c). **COSATI Field Group.** Field and Group assignments are to be taken from the 1964 COSATI Subject Category List. Since the majority of documents are multidisciplinary in nature, the primary Field/Group assignment(s) will be the specific discipline, area of human endeavor, or type of physical object. The application(s) will be cross-referenced with secondary Field/Group assignments that will follow the primary posting(s).
18. **Distribution Statement.** Denote public releasability, for example "Release unlimited", or limitation for reasons other than security. Cite any availability to the public, other than NTIS, with address, order number and price, if known.
- 19 & 20. **Security Classification.** Do not submit classified reports to the National Technical Information Service.
21. **Number of Pages.** Insert the total number of pages, including introductory pages, but excluding distribution list, if any.
22. **NTIS Price.** Leave blank.